



Design and Synthesis of High-Performance Nonlinear Optical  
Chromophores

by

Todd R. Ewy

A thesis submitted in partial fulfillment of the requirements for the  
degree of

Master of Science

University of Washington

2001

Department of Chemistry

# Table of Contents

	Page
List of Figures .....	ii
Chapter 1: Second-Order Nonlinear Optics and its Applications in Electro-Optic Modulators .....	1
1.1: Theoretical Background .....	1
1.1.1: Photonics, Electronics and the Motivation for EO Polymer Research .....	1
1.1.2: Inorganic Crystals versus Organic Polymers .....	7
1.2: Introduction and Theory of Nonlinear Optics .....	4
1.2.1: Microscopic Nonlinearity .....	5
1.2.2: Quantitative View of First Order Hyperpolarizability .....	10
1.2.3: Importance of Refractive Index .....	12
1.2.4: Extensive View of Electro-optic Effect .....	16
1.2.5: Exclusive View of Electro-optic Effect .....	17
1.2.6: Relating Molecular Hyperpolarizability to Macroscopic Electro-optic Activity .....	25
1.3: Electro-optic Polymeric Device Requirements .....	26
Notes to Chapter 1 .....	30
Chapter 2: The Importance of Chromophore-Chromophore Electrostatic Interactions and Their Impact on Nonlinear Optical Properties .....	32
2.1: Debye, London and the Electrostatic Interaction Models .....	32
2.2: Theories of Electro-optic Activity and Electrostatic Interactions .....	33
Notes to Chapter 2 .....	40
Chapter 3: Design and Synthesis of Chromophores Based on Reducing Intermolecular Electrostatic Interaction .....	41
3.1: Introduction .....	41
3.1.1: Motivation for Research .....	41
3.2: Design and Synthesis of the Chromophores .....	41
3.2.1: Design and Synthesis of the Triphenylamine Donor .....	41
3.2.2: Design and Synthesis of Chromophores Based On Triphenylamine Donor .....	43
3.3: Experimental Section .....	48
3.3.1: General Materials and Methods .....	48
3.3.2: Synthesis of Bis-(4-methoxyphenyl){4-[(triphenylphosphonium bromide) methyl]phenyl}amine .....	49
3.3.3: Synthesis of Chromophore 5 .....	51
3.3.4: Synthesis of Chromophore 6 .....	52
3.4: Conclusion .....	53
Notes to Chapter 3 .....	54
Bibliography .....	56

## List of Figures

	Page
Fig. 1.1: Refractive Index Ellipsoid.....	19
Fig. 1.2: Refractive Index of Ellipsoid under Electric Field Influence.....	20
Fig. 2.1: Plot of Electro-optic Coefficients versus Loading Density.....	37
Fig. 2.2: Electrostatic Interaction Axes.....	38
Fig. 3.1: Triphenylamine Donor Wittig Salt.....	42
Fig. 3.2: Synthetic Scheme for Triphenylamine Donor Wittig Salt .....	43
Fig. 3.2: Chromophores Utilizing Triphenylamine Donor .....	44
Fig. 3.3: Chromophores without Triphenylamine Donor for Comparison .....	45
Fig. 3.4: Synthetic Scheme for thieno[3,2-b]thiophene-dicarbaldehyde Bridge .....	46
Fig. 3.5: Synthetic Scheme for 2,3-thiophene[3,4-e]1,4-dioxane-5,7-dicarbaldehyde Bridge.....	46
Fig. 3.6: Synthetic Scheme for 2-dicyanomethylen-3-cyano-4,5,5-trimethyl- 2,5-dihydrofuran Acceptor.....	47
Fig. 3.7: Synthetic Scheme for Chromophore 5 .....	47
Fig. 3.8: Synthetic Scheme for Chromophore 6 .....	48
Fig. 3.9: <sup>1</sup> H NMR of Triphenylamine Donor Wittig Salt .....	51

## Acknowledgements

The author would like to thank the Department of Chemistry and Professor Larry Dalton for their generous support. He would also like to thank the members of the Dalton group for their synthetic insight and hard work. Finally, he would like to thank the U.S. Air Force for the opportunity to attend graduate school.

## **Chapter 1**

### **Second-Order Nonlinear Optics and its Applications in Electro-Optic Modulators**

#### **1.1 Theoretical Background**

##### **1.1.1 Photonics, Electronics and the motivation for EO polymer research**

For several years the world has relied on electronics for information processing. However, we are nearing the limits of traditional electronic signal processing and transmission. Optical technology will be required in order to gain processing rates above 50 GHz and a transmission distance greater than 1 meter. The optical technology is described as photonics, which is the analog of electronics. This means that photons, rather than electrons, will be used to acquire, store, transmit and process information. Many photonic applications are already in use. These include fiber-optic communication lines, diode laser sources, organic liquid-crystal displays and optical memories.<sup>1</sup>

There are many advantages of photonics over electronics. Optical switching, for example, occurs on a femtosecond time scale. No electronic process can come close to matching that time, but optical processes can. And with optical signals, there is no electrical and magnetic interference, so there is less crosstalk between channels.

In the past few years there has been a demand for more bandwidth. The explosion of multimedia applications through the Internet brought a requirement for higher bandwidth in order to run fast and smooth. Glass fibers are most commonly used to transmit data at high speeds because they have an inherent large bandwidth of more than 10THz. However, a decrease in the rate of transfer occurs at the electric-to-optic

signal conversion intersection between fibers. The data gets bottlenecked in these areas.<sup>2</sup>

Electro-optic modulators are a combination of electronics and photonics that help alleviate the bottleneck.

These modulators serve important fiber-optic and wireless functions, including: satellite receiver systems collecting high-quality rf signals that have been distributed long distances, connecting remote cellular radio systems with high-quality rf signals over long distances, and local area networks where low-distortion rf signals are needed.<sup>3</sup> Electro-optic modulators also find uses in other areas, such as frequency mixing, light modulation, optical logic, millimeter wave signal generation, optical beam steering, rf detection, phase control, power splitting, and wavelength division multiplexing (WDM).<sup>4,5</sup>

### **1.1.2 Inorganic Crystals vs Organic Polymers**

The field of nonlinear optics (NLO) took off with the coming of the laser. Laser beams have strong oscillating electrical fields that are capable of polarizing a medium nonlinearly corresponding to the field strength. The medium can then serve as a new optical field source with different frequencies and modified propagation qualities.

All forms of matter could exhibit nonlinear optical effects if the incoming optical field were strong enough. However, with today's laser sources, only a few materials display significant nonlinear optical effects.

There are basically two types of nonlinear optical materials, inorganic crystals and organic polymers, and classification depends on the origin of nonlinearity. The inorganic-crystal species, or ferroelectric crystals, include GaAs, KTiOPO<sub>4</sub> (KTP),

LiNbO<sub>3</sub> and LiTaO<sub>3</sub>. The nonlinear property of these materials comes from electrons shared by the bulk material, such as in metals and semiconductors. The electronic characteristics of the bulk medium determine the optical nonlinearity. The polymer materials include organic crystals and polymers. The nonlinearity in these materials comes from the molecular structure and geometrical arrangement of the molecules in the condensed medium.

Nalwa and Miyata list ten characteristics ideal nonlinear optical materials should have<sup>6</sup>:

1. Large nonlinear figure of merit for frequency conversion
2. High laser damage threshold
3. Fast optical response time
4. Wide phase matchable angle
5. Architectural flexibility for molecular design and morphology
6. Ability to process into crystals, thin films
7. Optical transparency (no absorption at fundamental and SH wavelengths)
8. Ease of fabrication
9. Nontoxicity and good environmental stability
10. High mechanical strength and thermal stability

Polymer materials have a few advantages over inorganic crystalline materials. Organic molecules can be synthesized, processed and integrated in ways inorganic crystals cannot be. This synthetic freedom allows researchers to optimize nonlinear



responses. Molecular materials also exhibit exceptional mechanical properties, thermal and chemical stability, optical transparency and high laser damage thresholds.

Inorganic crystals are based on positive and negative ions. The ionic lattice deforms relatively slowly in response to laser light interaction. This deformation leads to heat dissipation, which limits the cycle time of these devices. These resonant optical nonlinearities have a response time established by the lifetime of the excitation. On the other hand, polymer materials have large, nonresonant optical susceptibilities derived from ultrafast excitations and a large displacement of conjugated  $\pi$ -electrons. The nonlinearity is limited only by the width of the driving laser pulse.

Another advantage is that polymer materials have low dc dielectric constants around the order of 3 as compared to 28 for  $\text{LiNbO}_3$ , for example. This results in a minimization of phase mismatch between optical and electrical pulses allowing a large operating bandwidth modulation.<sup>5</sup> Electro-optic modulators have nearly the same phase velocities at optical and microwave frequencies. A few years ago, waveguide modulators were proven to operate at frequencies as high as 150 GHz.<sup>3</sup>

Other advantages include the ability of polymer materials to be deposited directly onto a number of substrates, even conforming to flexible substrates, which is not practical with  $\text{LiNbO}_3$ . Combine this with the ability to operate modulators at very low voltages ( $<1\text{V}$ ) compared to  $\text{LiNbO}_3$  modulators ( $\sim 5\text{V}$ ). All this adds up to why so much research and effort has been put forth in the search for high-performance polymeric electro-optic materials.

## 1.2 Introduction and Theory of Nonlinear Optics

### 1.2.1 Microscopic Nonlinearity

A linear response is simply the lowest-order approximation describing a process. A process is termed nonlinear if the response to an input physically changes the process itself. Nonlinear optics deals with the interactions between light waves and matter or light waves and other light waves. When electromagnetic radiation intermingles with a nonlinear optical material, the optical characteristics of the material change, which transforms the properties of the interacting light itself.

To describe nonlinear optical phenomena requires looking at the origin of electronic polarization. At the atomic level, the electromagnetic field  $E$  ( $E = \cos\omega t$ ) exerts a force  $F$  on an electron:

$$F = -eE \quad (1.1)$$

The original state is perturbed from its equilibrium position, and the electron density is displaced. This displacement gives rise to a charge separation or electron density polarization  $P$ :

$$P = -er \quad (1.2)$$

where  $r$  is the displacement of charge. The polarization is driven by the applied electric field, so it is easiest to picture the displaced system as a Lorenz Oscillator.<sup>7</sup> The electron acts as a harmonic oscillator bound to a nucleus by a spring with natural frequency  $\omega_0$ . Next, consider only the linear response in which the restoring force from the nucleus is approximated as linearly proportional to the displacement. The equation of motion is then written as a second order differential equation:

$$eE - m\omega_0^2 r = m \frac{d^2 r}{dt^2} + 2\Gamma \frac{dr}{dt} \quad (1.3)$$

The terms on the left side of the equation represent the Coulomb force and the restoring force. The right side contains a damping term with coefficient  $\Gamma$  to account for energy dissipation during the polarization. Solving the equation for the displacement  $r$  gives:

$$r = -\frac{e}{m} \frac{1}{\omega_0^2 - 2i\Gamma\omega - \omega^2} E_0 e^{i\omega t} + \text{c.c.} \quad (1.4)$$

Equation (1.4) reveals sinusoidal behavior in time with increasing displacement as the frequency of the field approaches the natural frequency of the oscillator. The atomic polarization is then written as:

$$P = \frac{e^2}{m} \frac{1}{\omega_0^2 - 2i\Gamma\omega - \omega^2} E_0 e^{i\omega t} + \text{c.c.} \quad (1.5)$$

This equation shows two things. First, the molecular polarization occurs sinusoidally with the identical frequency  $\omega$  to the driven field. Second, the amplitude of polarization is proportional to the strength of the applied field. Rearranging equation (1.5) into its real and imaginary parts gives:

$$P_{\text{Re}} = \frac{e^2}{m} \frac{\omega_0^2 - \omega^2}{(\omega_0^2 - \omega^2)^2 + 4\Gamma^2\omega^2} E_0 e^{i\omega t} + \text{c.c.} \quad (1.6)$$

$$P_{\text{Im}} = \frac{e^2}{m} \frac{2\Gamma\omega}{(\omega_0^2 - \omega^2)^2 + 4\Gamma^2\omega^2} E_0 e^{i\omega t} + \text{c.c.} \quad (1.7)$$

The real part, or in-phase part, of the polarizability shows that a new source of radiation with the same frequency as the fundamental wave evolves as the electromagnetic wave

propagates through the medium. The imaginary part reflects the out-of-phase polarizability and is attributed to the damping effect. This happens when a charge doesn't respond immediately to the applied field creating a phase difference between the polarization and the electric field results. Refractive index and birefringence are linear optical effects that result from linear polarization. Electron polarization, which occurs on the femtosecond time scale, is the fastest of all polarizations. For this reason organic nonlinearity is superior to inorganic crystals in terms of speed.

By similar reasoning the equation of motion describing nonlinear optical processes is derived after adding an anharmonic term  $ar^2$  to equation (1.3). This term acts as the first-degree correction to the nonlinear dependence of the restoring force on the electron displacement. Nearly all second order NLO effects are ascribed to this added term.

$$eE - m\omega_0^2 r = m \frac{d^2 r}{dt^2} + 2\Gamma \frac{dr}{dt} + ar^2 \quad (1.8)$$

By adding the anharmonic term, the exact solution to equation (1.8) can no longer be derived. The way around this is to assume that the anharmonic contribution to the total polarization is inconsequential. Then the solution to equation (1.8) can be approximated as a power series in charge displacement  $r$ . Accounting for the first two terms of the expansion:

$$r = r_1 + r_2 \quad (1.9)$$

The solution to  $r_1$  is practically identical to that of equation (1.3). Solving for the second term requires approximating  $ar^2$  as  $ar_1$ . Then equation (1.8) becomes a linear

differential equation, which leads to an exact solution in terms of a component at frequency  $2\omega$  and another at zero frequency or dc:

$$r_2 = r_2(2\omega) + r_2(0) + \text{c.c.} \quad (1.10)$$

The term  $r_2(2\omega)$  is expressed as:

$$r_2(2\omega) = -a \left( \frac{e}{m} \right)^2 E^2(\omega) \frac{e^{i2\omega t}}{(\omega_0^2 - 2i\Gamma\omega - \omega^2)(\omega_0^2 - 4i\Gamma\omega - 4\omega^2)} + \text{c.c.} \quad (1.11)$$

and

$$r_2(0) = -2a \left( \frac{e}{m} \right)^2 \frac{E(\omega)}{\omega_0^2} \frac{1}{(\omega_0^2 - 2i\Gamma\omega - \omega^2)} + \text{c.c.} \quad (1.12)$$

The  $r_2(2\omega)$  term shows in the exponential numerator that a new source of sinusoidal radiation at twice the original frequency  $\omega$  is being generated simply by including the second order correction term  $ar^2$  for the restoring force. This phenomenon is called second-harmonic generation (SHG). It is important to see that the amplitude of the SHG is proportional to the square of the applied electric field strength. The  $r_2(0)$  term shows that along with SHG, a frequency independent polarization is concurrently produced. This phenomenon is called optical rectification.

Up to this point both linear and nonlinear optical processes have been defined as the result of electron density redistribution after interaction with light waves. The linear effects are based on an approximation that the restoring force is linearly dependent on the electron displacement. In this case the electron redistribution is symmetric. When a higher order approximation to the displacement is made, as in the case of nonlinear

optical processes, the electron density redistribution is asymmetric. To get a non-zero  $\beta$  the molecule must have acentric symmetry.

A second way to approach optical nonlinear polarization is to express it as a power series of the field strength  $E$ :

$$p = \alpha E + \beta EE + \gamma EEE + \dots \quad (1.13)$$

where  $\alpha$  is the first-order linear polarizability,  $\beta$  is the first order molecular hyperpolarizability and  $\gamma$  is the second order hyperpolarizability. Substituting the electric field of a plane light wave,  $E = E_0 \cos(\omega t)$ , into equation (1.13) gives:

$$p = p_0 + \alpha E_0 \cos(\omega t - kr) + \frac{1}{2} \beta E_0^2 [1 + \cos(2\omega t - 2kr)] \\ + \gamma E_0^3 \left[ \frac{3}{4} \cos(\omega t - kr) + \frac{1}{4} \cos(3\omega t - 3kr) \right] \quad (1.15)$$

The third and fourth terms reveal new radiations are generated at frequencies  $2\omega$  and  $3\omega$ , respectively. The third term also shows a frequency independent dc polarization. Incidentally, the  $3\omega$  frequency is called third harmonic generation. Again, if  $\beta$  is to be non-zero, the molecule must be asymmetric.

Another way to present the NLO process is to examine how two different waves with electric fields  $E_1$  and  $E_2$  interact with NLO material electrons. Using two laser beams with frequencies  $\omega_1$  and  $\omega_2$ , the  $\beta$  in equation (1.14) becomes:

$$\beta E_1 \cos(\omega_1 t) E_2 \cos(\omega_2 t) \quad (1.16)$$

Equation (1.14) then looks like:

$$\beta E_1 \cos(\omega_1 t) E_2 \cos(\omega_2 t) = \frac{1}{2} \beta E_1 E_2 \cos[(\omega_1 + \omega_2)t] + \frac{1}{2} \beta E_1 E_2 \cos[(\omega_1 - \omega_2)t] \quad (1.17)$$

From this it is easy to see that polarizations occur at frequencies  $(\omega_1 + \omega_2)$  and  $(\omega_1 - \omega_2)$ . Radiation will be re-emitted at these frequencies with a dependence on the coefficient  $\beta$ . Notice that when  $\omega_1 = \omega_2$  the result is both SHG and optical rectification.

From the results of the previous equations it is seen that the interaction of light with NLO materials changes the subsequent properties of the light. Whether the process is looked at as electron distribution or wave-wave interaction, the responses both display optical nonlinearity.<sup>5</sup>

### 1.2.2 Quantitative View of First Order Hyperpolarizability

When the oscillating electric field of a light wave interacts with the electrons in an NLO medium, it perturbs the electrons from their ground state and causes oscillating currents in the molecule. The new electronic state is now a linear combination of the ground state and excited quantum states of the unperturbed system. The electric field is time dependent, which means that both the number of excited quantum states and the electron density distribution will fluctuate with time. Simply put, the oscillating electric field generates a time-dependent polarization. The fluctuating electron density can then be described by time-dependent perturbation theory.<sup>8</sup>

The time-dependent Schrödinger equation is:

$$H\Psi = i\hbar \partial\Psi/\partial t \quad (1.18)$$

The perturbing Hamiltonian is:

$$H' = -e\mathbf{r}E_0\sin\omega t \quad (1.19)$$

The overall Hamiltonian sums the unperturbed molecular Hamiltonian  $H_0$  and the interaction perturbation  $H'$ :

$$H = H_0 + H' = H_0 - e\mathbf{r}E_0 \sin\omega t \quad (1.20)$$

The  $\mathbf{r}$  term is the dipole moment operator summed over all electronic coordinates:

$$\mathbf{r} = \sum_{\alpha} \mathbf{r}_{\alpha} \quad (1.21)$$

The total molecular polarization, dipole plus induced dipole, is then written as:

$$\mathbf{p} = -e\langle\Psi|\mathbf{r}|\Psi\rangle \quad (1.22)$$

The next steps involve solving the Schrödinger equation, substituting the solution into equation (1.22) and collecting second order terms for the polarization equation. The first hyperpolarizability  $\beta$  is then derived:

$$\beta = \frac{1}{2\hbar^2} \sum_{e,e'} \langle g|\mu|e\rangle \langle e|\mu'|e'\rangle \langle e'|\mu'|g\rangle \left[ \frac{1}{(\Delta\omega_{e,g} - 2\omega)(\Delta\omega_{e',g} - \omega)} + \frac{1}{(\Delta\omega_{e,g} + \omega)(\Delta\omega_{e',g} - \omega)} + \frac{1}{(\Delta\omega_{e,g} + \omega)(\Delta\omega_{e',g} + 2\omega)} \right] \quad (1.23)$$

The  $\mu'$  term is the dipole moment difference operator defined as:

$$\langle n'|\mu'|n\rangle = \langle n'|\mu|n\rangle - \langle g|\mu|g\rangle \delta_{n'n} \quad (1.24)$$

The  $\delta_{n'n}$  term is the Kronecker delta, and  $\mu$  is the dipole moment operator. The dipole moment,  $\mu$ , describes the extent of charge separation. The transition dipole moment,  $\langle n'|\mu|n\rangle$ , determines the amount of mixing between the ground and excited states. When  $n' = n$ ,  $\delta_{n'n} = 1$ , and the result gives the difference between the excited state dipole moment and the ground state dipole moment. If  $n' \neq n$ ,  $\delta_{n'n} = 0$  giving the transition dipole moment from  $n$  to  $n'$ .



In 1977 Oudar used a simple two-state model to approximate  $\beta$  from the complete sum frequency generation perturbation calculation:

$$\beta = \frac{3e^2 \hbar^2 W f (\Delta\mu)}{2m [W^2 - (2\hbar\omega)^2] [W^2 - (\hbar\omega)^2]} \quad (1.25)$$

where

$$\Delta\mu = \mu_e - \mu_g \quad (1.26)$$

In equation (1.25)  $\beta$  is a function of the laser fundamental photon energy  $\omega$ , the electron charge  $e$  and mass  $m$ , the energy gap  $W$ , the oscillator strength  $f$  of the charge transfer transition in the molecule, and the change in dipole moment  $\Delta\mu$  resulting from that transition. To maximize  $\beta$  large  $\Delta\mu$  and  $f$  values are required. Alternatively, a small energy gap  $W$  near  $2\omega$  would also be desirable.<sup>9</sup>

Marder et al later reduced equation (1.25) to:

$$\beta = \frac{(\mu_{ee} - \mu_{gg})(\mu_{ge})^2}{(\Delta E_{ge})^2} \quad (1.27)$$

where  $(\mu_{ee} - \mu_{gg})$  is the difference between the excited-state and the ground state dipole moments. The coefficients  $\mu_{ge}$  and  $\Delta E_{ge}$  are the transition dipole moment and the optical (HOMO-LUMO) bandgap, respectively.<sup>10</sup>

### 1.2.3 Importance of Refractive Index

The index of refraction is the ratio of the speed of light in a vacuum to the speed of light in a specific medium. The refractive index of a material is an important component for determining the second-order nonlinear susceptibility  $\chi^{(2)}$ , which, along

with the first hyperpolarizability  $\beta$ , is needed to determine the second order nonlinear optical properties of a particular organic material.

Analogous to the atomic polarization, equation (1.13), the bulk polarization is written as:

$$P = \chi^{(1)}E + \chi^{(2)}EE + \chi^{(3)}EEE \quad (1.28)$$

where  $\chi^{(1)}$ ,  $\chi^{(2)}$ , and  $\chi^{(3)}$  are the macroscopic susceptibilities. The coefficient  $\chi^{(2)}$  is a third-rank tensor describing the second-order nonlinear optical susceptibility and is borne only of noncentrosymmetric mediums.

Optical radiation causes a disturbance in the electronic distribution of a molecule, which generates an electric field opposing the applied field. The total internal electric field  $D$  converts to:

$$D = E + 4\pi P \quad (1.29)$$

where  $4\pi P$  is the internal electric field generated by the polarization. The dielectric constant  $\epsilon$  is defined as the ratio of  $D$  to the applied field  $E$ , or:

$$\epsilon = \frac{E + 4\pi P}{E} \quad (1.30)$$

Rewrite equation (1.27) as:

$$P = \chi_{eff}E \quad (1.31)$$

The effective susceptibility,  $\chi_{eff}$ , is a function of the applied field representing the total bulk polarization. Substituting equation (1.30) into (1.29) exposes the dependence of the dielectric constant  $\epsilon$  on the polarization:

$$\epsilon(\omega) = 1 + 4\pi\chi_{eff}(\omega) \quad (1.32)$$

When working at optical frequencies and in the absence of dispersion, the dielectric coefficient of an isotopic material equals the square of the refractive index:

$$\eta^2(\omega) = \epsilon(\omega) = 1 + 4\pi\chi_{eff}(\omega) \quad (1.33)$$

If the optical field,  $E(\omega)$ , is modulated by a dc field,  $E(0)$ , the overall field  $E$  acting on the material is the sum of the two fields:

$$E = E(0) + E(\omega) = E(0) + E_0\cos(\omega t - kz) \quad (1.34)$$

Combining equation (1.34) with (1.28) gives (ignoring higher order terms):

$$\begin{aligned} P = & \chi^{(1)}[E(0) + E_0\cos(\omega t - kz)] + \chi^{(2)}[E(0) + E_0\cos(\omega t - kz)]^2 \\ & + \chi^{(3)}[E(0) + E_0\cos(\omega t - kz)]^3 \end{aligned} \quad (1.35)$$

Expanding equation (1.35) gives:

$$\begin{aligned} P = & \chi^{(1)}E_0\cos(\omega t - kz) + E^2(0) + 2\chi^{(2)}E(0)E_0\cos(\omega t - kz) + E_0^2\cos^2(\omega t - kz) \\ & + \chi^{(3)}E^3(0) + 3\chi^{(3)}E^2(0)E_0\cos(\omega t - kz) + 3\chi^{(3)}E(0)E_0^2\cos^2(\omega t - kz) \\ & + \chi^{(3)}E_0^3\cos^3(\omega t - kz) \end{aligned} \quad (1.36)$$

Next, reduce  $\cos^2$  and  $\cos^3$  terms. Then collect terms containing the frequency  $\omega$ :

$$\begin{aligned} P(\omega) = & \chi^{(1)}E_0\cos(\omega t - kz) + 2\chi^{(2)}E(0)E_0\cos(\omega t - kz) + 3\chi^{(3)}E^2(0)E_0\cos(\omega t - kz) \\ & + \frac{3}{4}\chi^{(3)}E_0^3\cos(\omega t - kz) \end{aligned} \quad (1.37)$$

Factor and rewrite equation (1.37) as:

$$P(\omega) = \chi_{eff}E(0)\cos(\omega t - kz) \quad (1.38)$$

Substitute the factored terms of  $\chi_{eff}E$  into equation (1.33) to get:

$$\eta^2(\omega) = 1 + 4\pi[\chi^{(1)} + 2\chi^{(2)}E(0) + 3\chi^{(3)}E^2(0) + \frac{3}{4}\chi^{(3)}E_0^2] \quad (1.39)$$

Designate the first-order linear refractive index as  $\eta_0^2$ , which comes from the linear polarization  $\eta_0 = 1 + 4\pi\chi^{(1)}$  to get:

$$\eta^2(\omega) - \eta_0^2 = 8\pi\chi^{(2)}E(0) + 12\pi\chi^{(3)}E^2(0) + 3\pi\chi^{(3)}E_0^2 \quad (1.40)$$

The left side of equation (1.40) can be rewritten as:

$$\eta^2(\omega) - \eta_0^2 = (\eta + \eta_0)(\eta - \eta_0) \approx 2\eta_0(\eta - \eta_0) \quad (1.41)$$

substitution of (1.41) into (1.40) gives:

$$\eta(\omega) = \eta_0 + \frac{4\pi\chi^{(2)}}{\eta_0} E(0) + \frac{6\pi\chi^{(3)}}{\eta_0} E^2(0) + \frac{3\pi\chi^{(3)}}{2\eta_0} E_0^2 \quad (1.42)$$

It is possible to show a direct relation between the nonlinear refractive index and the light intensity. The definition of light intensity in cgs units is:

$$E_0^2 = \frac{8\pi}{c\eta} I(\omega) \quad (1.43)$$

Substitute (1.42) into (1.41) getting:

$$\eta(\omega) = \eta_0 + \frac{4\pi\chi^{(2)}}{\eta_0} E(0) + \frac{6\pi\chi^{(3)}}{\eta_0} E^2(0) + \frac{12\pi^2\chi^{(3)}}{c\eta_0^2} I(\omega) \quad (1.44)$$

Rewrite equation (1.43) as:

$$\eta(\omega) = \eta_0(\omega) + \eta_1 E(0) + \eta_2(0) E^2(0) + \eta_2(\omega) I(\omega) \quad (1.45)$$

where  $\eta_1$  is the linear electro-optic (LEO) effect (the Pockels effect),  $\eta_2(0)$  is the quadratic electro-optic effect and  $\eta_2(\omega)$  shows the direct relationship between the nonlinear refractive index and the light intensity (Kerr effect). The  $\eta_1$  term given by:

$$\eta_1 = \frac{4\pi\chi^{(2)}}{\eta_0} \quad (1.46)$$

is proportional to the second-order nonlinear susceptibility  $\chi^{(2)}$ . This means that by applying a dc electric field to the medium, polarization will occur. This in turn alters the refractive indices, which changes the properties of the interacting light, such as a phase shift or a change of direction.<sup>11</sup>

The equation of the phase shift of the material is:

$$\Delta\phi = \frac{\pi\eta^3 rVL}{\lambda} \quad (1.47)$$

and

$$V_\pi = \frac{\lambda h}{\eta^3 rL} \quad (1.48)$$

where  $\Delta\phi$  is the electric field dependent phase shift of light passing through an electro-optic material,  $V$  is the applied electric field,  $h$  is the electrode spacing,  $\eta$  is the field-independent refractive index,  $r$  is the electro-optic coefficient of the material,  $L$  is the length of the material,  $\lambda$  is the wavelength of light and  $V_\pi$  is the voltage required to produce a  $\pi$  phase shift. The phase shift at given  $V$  and  $L$  is linearly proportional to  $\eta^3 r$ , which is also known as the figure of merit (FOM) for second-order NLO materials for light modulators.<sup>4</sup>

#### 1.2.4 Extensive View of Electro-optic Effect

The linear electro-optic effect, or Pockels effect, occurs when a static field induces a field-dependent change in the index of refraction at frequency  $\omega$ . It is directly observed only in noncentrosymmetric crystals.<sup>12</sup> It can be thought of as a three-wave

mixing process, where two waves at frequencies  $\omega_1$  and  $\omega_2$  interact to produce a third wave at frequency  $\omega_3$ . The second-order susceptibility has the form  $\chi^{(2)}(-\omega_3, \omega_1, \omega_2)$ . For the Pockels effect,  $\omega_2 = 0$ , giving  $\chi^{(2)}(-\omega_3, \omega_1, 0)$ .

There are many examples where the LEO effect plays an important role in technology, among them being signal transduction and optical switching.<sup>4,13,14,15</sup>

### 1.2.5 Exclusive View of Electro-optic Effect

Consider a light wave of arbitrary polarization traveling through a birefringent medium. Under Maxwell's equations, the optical field is seen as consisting of two mutually orthogonal linearly polarized electric field components. Each component of the light wave is commonly subjected to different refractive indices, which leads to birefringence. The indicatrix of refractive index, a potential energy surface that characterizes the refractive index of the traveling light, is used to explain this occurrence.

To derive the indicatrix, begin with the expression of the dielectric constant  $\epsilon$  in an isotropic medium. From equations (1.29) and (1.30),  $\epsilon$  relates is a second-rank tensor relating the electric field  $E$  and the dielectric displacement  $D$ . The vectors of  $D$ ,  $E$  and  $\epsilon$  can be expressed in matrix form:

$$\begin{pmatrix} D_x \\ D_y \\ D_z \end{pmatrix} = \begin{pmatrix} \epsilon_{11} & \epsilon_{12} & \epsilon_{13} \\ \epsilon_{21} & \epsilon_{22} & \epsilon_{23} \\ \epsilon_{31} & \epsilon_{32} & \epsilon_{33} \end{pmatrix} \begin{pmatrix} E_x \\ E_y \\ E_z \end{pmatrix} \quad (1.49)$$

If the medium is non-dispersive, the dielectric constant  $\epsilon$  tensor is symmetric. In the principal axes system all the off-diagonal elements are zero:

$$\begin{pmatrix} D_x \\ D_y \\ D_z \end{pmatrix} = \begin{pmatrix} \epsilon_{11} & 0 & 0 \\ 0 & \epsilon_{22} & 0 \\ 0 & 0 & \epsilon_{33} \end{pmatrix} \begin{pmatrix} E_x \\ E_y \\ E_z \end{pmatrix} \quad (1.50)$$

The diagonal elements are related to the refractive indices by:

$$\eta_x = \sqrt{\epsilon_{11}} \quad (1.51)$$

$$\eta_y = \sqrt{\epsilon_{22}} \quad (1.52)$$

$$\eta_z = \sqrt{\epsilon_{33}} \quad (1.53)$$

Zernike and Midwinter define the total electric energy density,  $W$ , in the medium by:

$$W = \frac{1}{8\pi} \left( \frac{D_x^2}{\eta_x^2} + \frac{D_y^2}{\eta_y^2} + \frac{D_z^2}{\eta_z^2} \right) \quad (1.54)$$

Simplify equation (1.53) with the following relationship:

$$x = \frac{D_x}{\sqrt{8\pi W}}, \text{ similarly for } y \text{ and } z \quad (1.55)$$

to get:

$$\frac{x^2}{\eta_x^2} + \frac{y^2}{\eta_y^2} + \frac{z^2}{\eta_z^2} = 1 \quad (1.56)$$

This is the equation for an ellipse. The elliptical axes are parallel to the principal directions in the medium. The incident light of wave-vector  $S$  has a fundamental frequency  $\omega$ . The two orthogonal polarization components are parallel to  $(I \cos \theta + K \sin \theta)$  and  $J$ , where  $I$ ,  $J$  and  $K$  are unit vectors in the molecular  $x$ ,  $y$  and  $z$  directions.

The first orthogonal component is defined as  $\eta_0$ , which is independent of the propagation

direction, normal to  $S$  and parallel to  $J$ . The second component is termed  $\eta_e$ . It is normal to both  $J$  and  $S$  and is dependent on the angle of inclination,  $\theta$ , of the incident beam with the optical axis. A positive uniaxial medium results, when, in equation (1.55),  $\eta_x = \eta_y \neq \eta_z$ . The refractive-index ellipsoid for this type of medium is shown in Fig. 1.1.

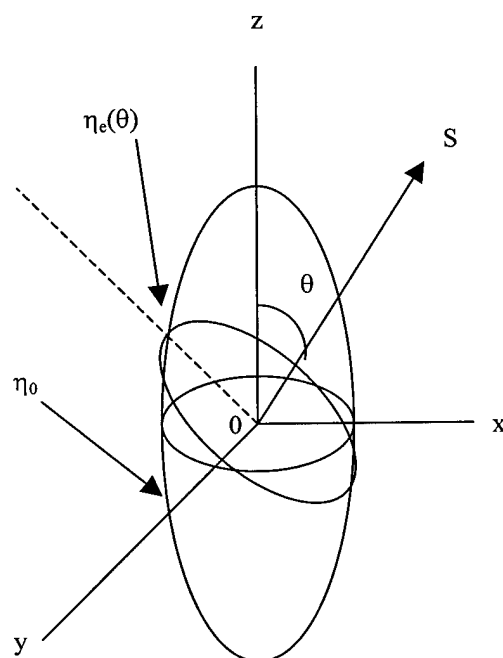


Fig. 1.1 Refractive index of uniaxial medium, where  $S$  is the direction of light propagation,  $\eta_0$  is the refractive index normal to  $S$  and parallel to  $J$ ,  $\eta_e$  is the refractive index normal to both  $S$  and  $J$ .

Applying an electric field to the nonlinear material alters the polarization susceptibility and the refractive index. On the molecular scale, the electron density is rearranged anisotropically. The overall effect of the rearrangement is a change in the shape or rotations to the ellipse. Either effect gives new values for the refractive indices.



This means that a beam of polarized light will have its plane of polarization rotated according to the strength and direction of the applied field subsequently changing the velocity and possibly the direction of the light. This is shown in Fig. 1.2.

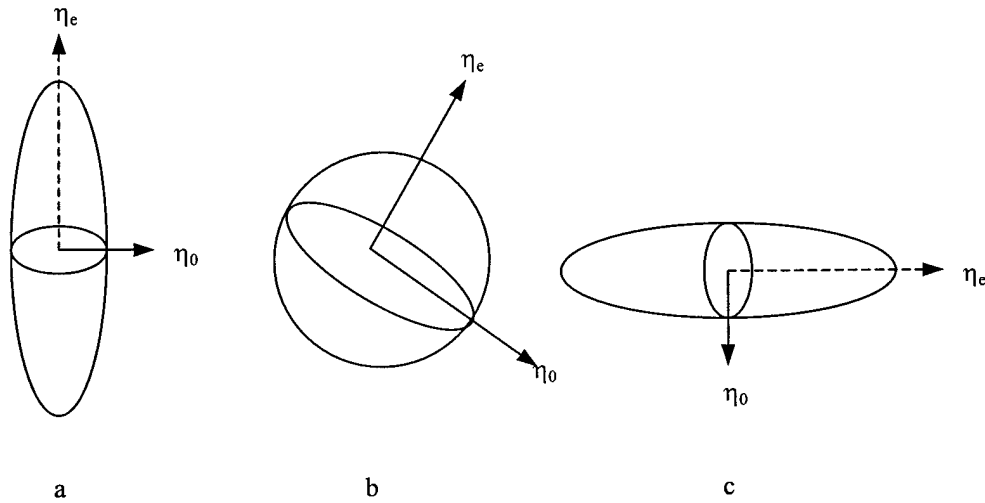


Fig. 1.2 Refractive index of an ellipsoid in (a) the absence of an applied electric field, (b) a medium field and (c) a strong field

Due to the applied electric field, additional math terms are needed for a complete description of the ellipsoid. Equation (1.55) becomes:

$$\left(\frac{1}{\eta^2}\right)_1 x^2 + \left(\frac{1}{\eta^2}\right)_2 y^2 + \left(\frac{1}{\eta^2}\right)_3 z^2 + 2\left(\frac{1}{\eta^2}\right)_4 yz + 2\left(\frac{1}{\eta^2}\right)_5 xz + \left(\frac{1}{\eta^2}\right)_6 xy = 1 \quad (1.57)$$

and

$$\begin{pmatrix} \Delta(\eta^2)_1^{-1} \\ \Delta(\eta^2)_2^{-1} \\ \Delta(\eta^2)_3^{-1} \\ \Delta(\eta^2)_4^{-1} \\ \Delta(\eta^2)_5^{-1} \\ \Delta(\eta^2)_6^{-1} \end{pmatrix} = \begin{pmatrix} r_{11} & r_{12} & r_{13} \\ r_{21} & r_{22} & r_{23} \\ r_{31} & r_{32} & r_{33} \\ r_{41} & r_{42} & r_{43} \\ r_{51} & r_{52} & r_{53} \\ r_{61} & r_{62} & r_{63} \end{pmatrix} \begin{pmatrix} E_1 \\ E_2 \\ E_3 \end{pmatrix} \quad (1.58)$$

Let  $x$ ,  $y$  and  $z$  be parallel to the principal dielectric axes of the medium. In the absence of an electric field, equation (1.58) turns into:

$$\frac{1}{\eta_0^2}(x^2 + y^2) + \frac{1}{\eta_e^2}z^2 = 1 \quad (1.59)$$

The expression relating the change in the refractive index as a function of the applied electric field to the new and old values of the refractive indices is:

$$\Delta\left(\frac{1}{\eta^2}\right)_i = \sum_{j=1}^3 r_{ij} E_j \quad \text{for } i = 1 \text{ to } 6 \quad (1.59)$$

The  $r_{ij}$  quantity in the contracted form of notation can be replaced by  $r_m$ . The relationship between the contracted and uncontracted suffixes is:

$$\begin{aligned} ij &\rightarrow m \\ 11 &\rightarrow 1 \\ 22 &\rightarrow 2 \\ 33 &\rightarrow 3 \\ 23 \text{ or } 32 &\rightarrow 4 \\ 31 \text{ or } 13 &\rightarrow 5 \\ 12 \text{ or } 21 &\rightarrow 6 \end{aligned} \quad (1.60)$$

The  $r_{ij}$  matrix is under the same symmetry constraints as the second-order NLO coefficient and is directly related to it.

As an example of how an applied electric field changes the refractive index of a uniaxial medium, consider dipolar chromophores in an amorphous polymer film. Under

the influence of a strong electric field, the chromophores will align parallel to the poling direction, which is perpendicular to the film. The point group of the poled film is  $\infty mm$ , or  $C_{\infty v}$ . The symmetry operations have an infinite-fold rotation about the poling field direction and an infinite number of mirror planes including the poling field direction.

The electro-optic coefficient tensor  $r_{ij}$  becomes:

$$\Delta\left(\frac{1}{\eta^2}\right)_i = \sum_{j=1}^3 r_{ij} E_j = \begin{vmatrix} 0 & 0 & r_{13} \\ 0 & 0 & r_{23} \\ 0 & 0 & r_{33} \\ 0 & r_{42} & 0 \\ r_{51} & 0 & 0 \\ 0 & 0 & 0 \end{vmatrix} \begin{vmatrix} E_1 \\ E_2 \\ E_3 \end{vmatrix} \quad (1.61)$$

There will be two pairs of equivalent indices due to the symmetry of the medium. In the absence of absorption, under the Kleinman symmetry constraint,  $r_{13} = r_{23} = r_{42} = r_{51}$  giving two independent components of the electro-optic coefficient  $r_{\parallel} = r_{33}$  and  $r_{\perp} = r_{13}$ , which are parallel and perpendicular to the polar axis, respectively.

For a dc field applied in the z direction:

$$\Delta\left(\frac{1}{\eta^2}\right)_1 = \Delta\left(\frac{1}{\eta^2}\right)_2 = \Delta\left(\frac{1}{\eta_0^2}\right) = r_{13} E_z \quad (1.62)$$

and

$$\Delta\left(\frac{1}{\eta^2}\right)_3 = \Delta\left(\frac{1}{\eta_e^2}\right) = r_{33} E_z \quad (1.63)$$

Now equation (1.63) becomes:

$$\left(\frac{1}{\eta_0^2} + r_{13} E_z\right)(x^2 + y^2) + \left(\frac{1}{\eta_e^2} + r_{33} E_z\right)z^2 = 1 \quad (1.64)$$

In general  $r_{13}$  is smaller than  $r_{33}$ , and in highly anisotropic materials,  $r_{13}$  approaches zero.

An alternative derivation of the light output phase difference comes from the reflection technique<sup>16</sup>:

$$I_{\text{output}} = \Delta I \sin^2 \frac{\Psi_{\text{sp}}}{2} \quad (1.65)$$

where  $\Delta I$  is the intensity contrast,  $I_{\text{max}} - I_{\text{min}}$ , and  $\Psi_{\text{sp}}$  is the phase difference between s- (TE) and p- (TM) polarized waves. Note that the incident beam is polarized 45 degrees, thus intensities for both TE and TM are identical. The equation for the phase difference is written:

$$\Psi_{\text{sp}} = \Psi_{\text{sp}}^0 + \delta\Psi_{\text{sp}} \quad (1.66)$$

where  $\Psi_{\text{sp}}^0$  is the phase retardation due to birefringence and  $\delta\Psi_{\text{sp}}$  is the induced phase retardation due to the Pockels effect (or LEO effect, in this regard, Kerr's optical effect is assumed to contribute to the modulation neglectably in contrast to the Pockels effect.)

$$\delta\Psi_{\text{sp}} = \delta\Psi_p - \delta\Psi_s \quad (1.67)$$

The term  $\delta\Psi_p$  is the induced phase retardation of TM polarization and  $\delta\Psi_s$  is the induced phase shift of TE polarization. The incident wave beam is defined as:

$$\Psi = \frac{2\pi}{\lambda} \eta L \quad (1.68)$$

where  $\eta$  is the refractive index,  $L$  is the optical path length and  $\lambda$  is the free space wavelength of the modulated beam. Introduce a small phase difference to equation (1.68):

$$\delta\Psi = \delta\left(\frac{2\pi}{\lambda}\eta L\right) \quad (1.69)$$

$$\delta\Psi = \frac{2\pi}{\lambda}(\eta\delta L + L\delta\eta) \quad (1.70)$$

When  $L = \frac{2d}{\cos\alpha}$ , where  $d$  is the electrode distance, the derivative of  $L$  is:

$$\delta L = \frac{2d \sin\alpha}{\cos^2\alpha} \delta\alpha \quad (1.71)$$

By Snell's law,  $\sin\theta = \eta_g \sin\theta_g = \eta \sin\alpha$ , where  $\theta$  is the angle of the laser beam irradiating on the glass surface from air ( $\eta=1$ ),  $\eta_g$  is the refractive index of the glass substrate,  $\theta_g$  is the refracting angle in the glass,  $\eta$  is the refractive index of the polymer and  $\alpha$  is the refracting angle in the polymer media. For fixed angle measurements,

$$0 = \delta \sin\theta = \delta\eta \sin\alpha = \delta(\eta \sin\alpha) \quad (1.72)$$

$$0 = \eta(\delta\alpha) \cos\alpha + (\delta\eta) \sin\alpha \quad (1.73)$$

$$\delta\alpha = -\frac{\sin\alpha}{\eta \cos\alpha} \delta\eta \quad (1.74)$$

Substitute (1.74) into (1.71) to get:

$$\delta L = \frac{2d \sin\alpha}{\cos^2\alpha} \left(-\frac{\sin\alpha}{\eta \cos\alpha} \delta\eta\right) = -\frac{2d \sin^2\alpha}{\eta \cos^3\alpha} \delta\eta \quad (1.75)$$

Combine equations (1.75) and (1.70) to get:

$$\delta\Psi = \frac{2\pi}{\lambda} \left( L\delta\eta - \eta \times \frac{2d \sin^2\alpha}{\eta \cos^3\alpha} \delta\eta \right) = \frac{2\pi}{\lambda} \left( L - \frac{2d \sin^2\alpha}{\cos^3\alpha} \right) \delta\eta \quad (1.76)$$

Recall equation (1.66),  $\delta\Psi_{sp} = \delta\Psi_p - \delta\Psi_s$ .

$$\delta\Psi_{sp} = \frac{2\pi}{\lambda} \left( L - \frac{2d \sin^2 \alpha}{\cos^3 \alpha} \right) (\delta\eta_p - \delta\eta_s) \quad (1.77)$$

Substitute (1.77) into (1.65). The final output intensity is then given by:

$$I_{\text{output}} = \Delta I \sin^2 \left[ \frac{\delta\Psi_0}{2} + \frac{\pi}{\lambda} \left( L - \frac{2d \sin^2 \alpha}{\cos^3 \alpha} \right) (\delta\eta_p - \delta\eta_s) \right] \quad (1.78)$$

### 1.2.6 Relating Molecular Hyperpolarizability to Macroscopic Electro-optic Activity

The equation for the macroscopic polarization is given by equation (1.28):

$$P = \chi^{(1)}E + \chi^{(2)}EE + \chi^{(3)}EEE \quad (1.28)$$

The second-order nonlinear susceptibility,  $\chi^{(2)}$ , is zero for centrosymmetric materials.

The expression relating macroscopic  $\chi^{(2)}$  to  $\beta$  is:

$$\chi^{(2)} = N\beta f(\omega_1)f(\omega_2)f(\omega_3)\Gamma(\Omega) \quad (1.79)$$

where  $N$  is the molecular number density and  $f(\omega_i)$  are the local field factors due to intermolecular interactions. The  $f(\omega_i)$  terms are derived from the Onsager correction equation:

$$f(\omega_i) = \frac{[(\epsilon^i)_\infty + 2](\epsilon_\omega)}{[(\epsilon^i)_\infty + 2\epsilon_\omega]} \quad (1.80)$$

For an isotropic distribution of chromophores,  $\chi^{(2)}$  equals zero. An orientation factor,  $\Gamma(\Omega)$ , provides the projection of  $\beta$  onto the macroscopic framework established by the direction of the applied poling field.

To observe second-order nonlinear optical effects, externally applied dc fields are required to induce  $C_{\infty v}$  cylindrical polar symmetry. Under the Kleinman restrictions only two independent  $\chi^{(2)}$  tensor components are nonzero:

$$\chi_{zzz}^{(2)} = N\beta f(\omega_1)f(\omega_2)f(\omega_3)\langle \cos^3 \theta \rangle \quad (1.81)$$

and

$$\chi_{zzx}^{(2)} = N\beta f(\omega_1)f(\omega_2)f(\omega_3)\langle \cos \theta \rangle \langle \cos^2 \theta \rangle \quad (1.82)$$

The dc field removes the orientational averaging replacing  $\Gamma(\Omega)$  with  $\langle \rangle$ . The  $\theta$  term is the angle between the dipole moment of the nonlinear molecule (parallel to  $\beta$ ) and the dc poling field,  $E$ . The macroscopic electro-optic coefficient,  $r_{33}$ , is related to  $\beta$  (expressed in esu units) by:

$$r_{33} = \frac{2N\beta f(\omega_1)f(\omega_2)f(\omega_3)\langle \cos^3 \theta \rangle}{(n_e)^4} \quad (1.83)$$

where  $\langle \cos^3 \theta \rangle$  is the acentric ordering parameter. The following chapter begins with equation (1.83) and deals exclusively with the details of interactions between chromophores.

### 1.3 Electro-optic Polymeric Device Requirements

A few ideas from nonlinear optical material theory are needed in order to fabricate viable devices. The materials should have high  $r_{33}$  values, low optical loss, good thermal and chemical stability during operating conditions, and the ability to maintain polar alignment.

For practical reasons, electro-optic polymeric devices need to have operational voltages,  $V_\pi$ , of less than three volts. Equation (1.83) shows that high- $\beta$  chromophores are needed to produce high  $r_{33}$  values. Many disciplinary fields, such as optical, electrical and molecular engineering, chemical theorists and synthetic chemists combine to create, test and integrate novel NLO materials into useful devices. Over the years many high- $\beta$  chromophores have been produced, but they do not always lead to high macroscopic  $r_{33}$  values. One fundamental reason was provided by Dalton *et. al.*, who showed that electrostatic interactions between high- $\beta$  chromophores could sometimes limit the correlation between micro- and macroscopic optical nonlinearity.<sup>4</sup> The electrostatic interaction produces chromophore aggregates which do not contribute to the electro-optic effect when the chromophore loading density reaches a certain level. Therefore, the molecular architecture of the chromophores is very important in order to produce high- $\beta$  chromophores that won't clump together under optional loading conditions.

It is important for devices to have as little optical loss as possible. Optical loss is classified either as loss due to absorption of light or due to scattering of light. Loss by absorption has two causes. The first arises in the absorption tail of the interband (HOMO-LUMO) absorption and the second is due to absorption caused C-H group vibrations. However, if needed, the hydrogens of the C-H groups can be replaced with fluorine, and a large difference between the operating wavelength and interband absorption maximum can be maintained. This means that the proper chromophore and polymer design can keep absorption loss to a minimum. The light should have a total



attenuation of less than 1 dB/cm. This means the chromophores should not absorb light at operational wavelengths. Since many high- $\beta$  chromophores have absorption maxima above 650 nm,<sup>18,19</sup> they are unfit for device application.

Optical loss due to scattering is a different problem. A major contributor is the heterogeneity of the index of refraction in materials. This heterogeneity can arise from chromophore/polymer incompatibility or process-induced losses, such as spin casting, electric field poling, waveguide fabrication, and/or cladding deposition of thin films. Another area of optical loss arises from impedance mismatch between silica fibers and polymeric waveguides.<sup>4</sup>

The thermal and chemical stability of chromophores and polymers is essential for both the fabrication and operation of devices. There seems to be a trade-off between high- $\beta$  chromophores and high thermal stability. For instance, increasing the  $\pi$ -conjugation length gives higher  $\beta$  values but lowers the decomposition temperature. It has been shown that the thermal stability of electro-optic activity can be correlated with the difference between the operating temperature and the glass transition temperature ( $T_g$ ) of the chromophore/polymer composite.<sup>19,20</sup>

Stabilizing the polar alignment of the polymeric electro-optic materials critical for device operation. Electro-optic activity must be stable for both long-term operation at temperatures up to 125 °C and short-term operation at temperatures nearing 200 °C. There are currently two methods to achieve this. The first is to utilize high- $T_g$  polymers in chromophore/polymer composite materials. The second method involves covalently coupling the chromophore and polymer, then inducing some type of lattice hardening

near the end of the poling process. The chromophores are either tethered to the polymer backbone,<sup>20,21,22</sup> or incorporated directly into the polymer backbone.<sup>23,24</sup> The purpose of this study was to develop high- $\beta$  chromophores with improved thermal and chemical stability and potentially less electrostatic interaction by way of a new donor.

## Notes to Chapter 1

1. Eldada, L., Blomquist, R., Shacklette, L.W., McFarland, M.J., *Opt. Eng.*, 2000, **39**, 596-609.
2. Chen, A., Ph.D. Dissertation, 1998, Department of Electrical Engineering, University of Southern California.
3. Tang, S., Shi, Z., An, D., Sun, L., Chen, R.T., *Opt. Eng.*, 2000, **39**, 680-688.
4. Dalton, L.R., Steier, W.H., Robinson, B.H., Zhang, C., Ren, A., Garner, S., Chen, A., Londergan, T., Irwin, L., Carison, B., Leonard, F., Phelan, G., Kincaid, C., Amend, J., Jen, A., *J. Mater. Chem.*, 1999, **9**, 1905-1920.
5. Zhu, J., Ph.D. Thesis, University of Southern California, 1997.
6. Nalwa H.S., Miyata, S. Nonlinear Optics of Organic Molecules and Polymers, CRC Press, New York, 1997, p. 129.
7. Zernike, F., Midwinter, J.E. Applied Nonlinear Optics, Wiley, New York, 1973, p. 3ff.
8. Ward, *J. Rev. Mod. Phys.*, 1965, **37**, 1.
9. Nicoud, J.F., Twieg, R.J. in Nonlinear Optical Properties of Organic Molecules and Crystals, eds. D.S. Chemla, J. Zyss, Vol. 1, Academic Press, Orlando, 1989, p. 232.
10. Marder, S.R., Beretan, D.N., and Cheng, L.T., *Science*, 1991, **252**, 103.
11. Prasad, P.N., Williams, D.J. Introduction to Nonlinear Optical Effects in Molecules and Polymers, Wiley, New York, 1991.
12. Dalton, L.R., Steier, W.H., Robinson, B.H., Zhang, C., Ren, A., Garner, S., Chen, A., Londergan, T., Irwin, L., Carlson, B., Fifield, L., Phelan, G., Kincaid, C., Amend, J., Jen, A., *J. Mater. Chem.*, 1999, **9**, 1905-1920.
13. Pugh, D., Morley, J.O. in Nonlinear Optical Properties of Organic Molecules and Crystals, eds. D.S. Chemla, J. Zyss, Vol. 1, Academic Press, Orlando, 1989, p. 205.
14. Dalton, L.R., Kirk-Othmer Encyclopedia of Chemical Technology, 4<sup>th</sup> edn., Vol. 17, Wiley, New York, 1996, p. 287.
15. Dalton, L.R., Harper, A.W., Wu, B., Ghosn, R., Laquinadanum, J., Liang, Z., Hubbel, A., Xu, C., *Adv. Mater.*, 1995, **7**, 519.

16. Nalwa H.S., Miyata, S. Nonlinear Optics of Organic Molecules and Polymers, CRC Press, New York, 1997, p. 406.
17. Zhang, Y., Jen, A.K.Y., Chen, T., Liu, Y., Zhang, X., Kenney, J.T., *SPIE*, 1996, **3006**, 372.
18. Boldt, P., Bourhill, G., Brauchle, C., Jim, Y., Kammler, R., Muller, C., Rase, J., Wichern, J., *J. Chem. Commun.*, 1996, 793.
19. Burland, D.M., Miller, R.D., Walsh, C.A., *Chem. Rev.*, 1994, **94**, 31.
20. Marks, T.J., Ratner, M., *Angew. Chem., Int. Ed. Engl.*, 1995, **34**, 155.
21. Xu, C., Wu, B., Todorova, O., Dalton, L.R., Shi, Y., Ranon, P.M., Steier, W.H., *Macromolecules*, 1993, **26**, 5303.
22. Shi, Y., Ranon, P.M., Steier, W.H., Xu, C., Wu, B., Dalton, L.R., *App. Phys. Lett.*, 1993, **63**, 2168.
23. Wu, B., Xu, C., Dalton, L.R., Kalluri, S., Shi, Y., Steier, W.H., *Mater. Res. Soc. Symp. Proc.*, 1994, **328**, 529.
24. Xu, C., Wu, B., Becker, M.W., Dalton, L.R., Ranon, P.M., Shi, Y., Steier, W.H., *Chem. Mater.*, 1993, **5**, 1439.

## Chapter 2

### The Importance of Chromophore-Chromophore Electrostatic Interactions and Their Impact on Nonlinear Optical Properties

#### 2.1. Debye, London and the Electrostatic Interaction Models

The work of Debye in the late 1930s<sup>1</sup> resulted in theories still used today to describe the behavior of noninteracting dipoles under the influence of an external electric field. Chromophores in a polymer matrix are viewed as independent particles. These independent particles form the gas phase model of macroscopic optical nonlinearity, which, until recently, was universally accepted as the calculation standard for the  $\mu\beta/M_w$  figure of merit. Here  $\mu$  is the chromophore ground-state dipole moment,  $\beta$  is the first hyperpolarizability and  $M_w$  is the molecular weight of the nonlinear optically-active moiety (chromophore). Recently developed chromophores, such as FTC<sup>2</sup> and CZC<sup>3</sup>, with high  $\mu\beta$  values on the order of  $10^{-44}$  esu and  $r_{33}$  values ranging from 55 to 84 pm V<sup>-1</sup>, have surpassed lithium niobate ( $r_{33} \approx 30$  pm V<sup>-1</sup>). Under the gas phase model, the macroscopic electro-optic activity was predicted to scale as  $\mu\beta/M_w$ . However, with this scaling, the bulk nonlinear optical coefficients from high- $\beta$  chromophores are well below the values expected from the chromophore hyperpolarizabilities. The gas phase model appears to be inadequate for high- $\beta$  chromophores, which has led to the examination of other theories exploiting electrostatic interactions.

Chromophores consist of aromatic and  $\pi$ -conjugated subunits. As the polarization of the electron cloud increases, the strength of electrostatic interactions also generally increases. Chromophores, then, will have greater electrostatic interactions than

saturated molecules. The interactions between neighboring chromophores alter the electron density distribution in each molecule, which changes the molecule's chemical, physical and photophysical properties. Thus, electrostatic interactions must be taken into account.

The work of Fritz London in the 1930s<sup>4</sup> led to the ability to calculate, using statistical mechanics, electrostatic interaction contributions. He showed that the attraction between molecules varied with distance,  $r$ , as  $r^{-6}$ . Molecules with small dipole moments and polarizabilities have fairly small electrostatic interactions. This means that other interactions are competing, such as solute-solvent, solute-solute, and H-bonding interactions. For these molecules the London forces are short-ranged. But as the dipole moments and polarizabilities increase, the solute-solute interactions dominate, and the overall electrostatic interactions are longer ranged. It has been shown recently that large dipole moments and polarizabilities of chromophores result in strong London forces.<sup>5,6,7</sup> These forces are largely responsible for the disparity between high- $\beta$  chromophores and low electro-optic coefficients. This chapter will show how London theory is used both to define electro-optic activity and reveal the importance of chromophore structure to optical nonlinearity.

## 2.2 Theories of Electro-optic Activity and Electrostatic Interactions

Begin with equation (1.83), where  $\eta_e$  is the extraordinary refractive index. The  $r_{33}$  term is in esu units, where  $1\text{cm}^2/\text{esu} = 4.19 \times 10^{-4} \text{ m/V}$ .

$$r_{33} = \frac{2N\beta f(\omega_1)f(\omega_2)f(\omega_3)\langle \cos^3 \theta \rangle}{(n_e)^4} \quad (1.83)$$

The acentric ordering parameter,  $\langle \cos^3\theta \rangle$ , defines the competition between the chromophore/electric field interactions and the thermal randomization energy. It is also possible to estimate the electro-optic coefficient as:

$$r_{33} = 3 \left( \frac{\eta_0}{\eta_e} \right)^4 (r_{13}) \quad (2.1)$$

but this does not always hold true with electric field poling<sup>8</sup> and hardly ever holds true for laser-assisted poling.

To determine  $\langle \cos^3\theta \rangle$ , start with the Gibbs distribution function:

$$G(\Omega, E_p) = \frac{\exp[-U(\Omega, E_p)]}{kT} \quad (2.2)$$

The term  $[-U(\Omega, E_p)]$  represents the potential energy of the chromophore dipole. It is composed of two energy contributions. The first,  $U_0$ , is from the intermolecular interactions in the local environment of the chromophore. The second,  $U_1$ , arises from the chromophore/electric poling field interactions. Using bold type to represent vector and tensor quantities,  $U_1$  is expressed as:

$$U_1 = -\boldsymbol{\mu} \cdot \mathbf{F} - \left( \frac{1}{2} \right) \boldsymbol{\alpha} \cdot \mathbf{F} \cdot \mathbf{F} \quad (2.3)$$

where  $\mathbf{F}$  is the local electric field at the chromophore. A typical approximation for  $\langle \cos^3\theta \rangle$  involves neglecting the chromophore-chromophore intermolecular electrostatic interactions ( $U_0$ ) along with the polarizability term. This gives:

$$U_1 = \mu f_p E_p \cos\theta \quad (2.4)$$

where  $\mu$  is the chromophore dipole moment,  $E_p$  is the magnitude of the applied electric poling field, and  $f_p E_p$  is the effective poling field felt by the chromophore. The term  $f_p E_p$  is equal to  $V/h$ , where  $V$  is the voltage of the applied poling field and  $h$  is the film thickness. Now the order parameter can be computed according to statistical mechanics:

$$\langle \cos^x \theta \rangle = L_x \left( \frac{\mu f_p E_p}{kT} \right) = \frac{\int \exp \left( \frac{-\mu f_p E_p \cos \theta}{kT} \right) \cos^x \theta \sin \theta d\theta}{\int \exp \left( \frac{-\mu f_p E_p \cos \theta}{kT} \right) \sin \theta d\theta} \quad (2.5)$$

where the integrals are evaluated from  $\theta = 0$  to  $180^\circ$ . The term  $L_x(\mu f_p E_p/kT)$  represents Langevin functions, which are related to the averaged values of the Legendre polynomials  $\langle P_x(\cos \theta) \rangle$ . Let  $x = (\mu f_p E_p/kT)$  to get:

$$\langle \cos \theta \rangle = L_1(x) = \coth(x) - (1/x) = \langle P_1(\cos \theta) \rangle \quad (2.6)$$

$$\langle \cos^2 \theta \rangle = L_2(x) = 1 + (2/x^2) - (2/x)\coth(x) = (1/3)[2\langle P_2(\cos \theta) \rangle + 1] \quad (2.7)$$

$$\begin{aligned} \langle \cos^3 \theta \rangle &= L_3(x) = (1 + 6/x^2)\coth(x) - (3/x)(1 + 2/x^2) \\ &= (1/5)[2\langle P_3(\cos \theta) \rangle + 3\langle P_1(\cos \theta) \rangle] \end{aligned} \quad (2.8)$$

The Langevin functions can be expanded in a power series:

$$L_1(x) = (x/3) - (x^3/45) + (2x^5/945) + \dots \quad (2.9)$$

$$L_3(x) = L_1(x)(1 - 6/x^2) - (2/x) = (x/5) - (x^3/105) + \dots \quad (2.10)$$

Assume  $\mu f_p E_p \ll kT$  and use only the first terms of the power series to get:

$$\langle \cos^3 \theta \rangle = x/5 = \mu f_p E_p / 5kT \quad (2.11)$$



The number density,  $N$ , has been defined by workers at IBM, Lockheed-Martin<sup>9</sup>, Akzo<sup>10</sup> and elsewhere in terms of the weight fraction of the chromophore in the polymer,  $w$ . This leads to the relationship between  $r_{33}$  and  $\beta$ :

$$r_{33} = \frac{2w\rho N_A f_p f_\omega^2 E_p}{15kT\eta^4} \left( \frac{\mu\beta}{M_w} \right) \quad (2.12)$$

where  $N_A$  is Avagadro's number,  $\rho$  is the density of the nonlinear polymer system,  $M_w$  is the molecular weight of the chromophore and  $T$  is the poling temperature. This suggests that the electro-optic coefficient should increase linearly with the chromophore number density (loading). However, this has not been observed with experimentation. For chromophores with large polarizabilities and dipole moments, the electro-optic coefficient does not increase linearly. In fact, many of these chromophores exhibit maximum peaks. The chromophore-chromophore electrostatic interactions are responsible for the deviation. Figure 2.1 represents this.

Dalton et. al. have developed a theoretical model that successfully predicts the trends in the electro-optic coefficient as the loading density and molecular structure change.<sup>5</sup> Dalton's model uses ordering and disordering forces as components of the acentric ordering parameter  $\langle \cos^3\theta \rangle$ . With so many intermolecular electrostatic interactions between chromophores, the problem is a many-body problem. Statistical mechanics is the most logical way to approach the problem, although it would require solving a tremendous number of rotational matrices that relate the chromophores to each other and to the electric poling field. The integrals of equation (2.5) would have to be

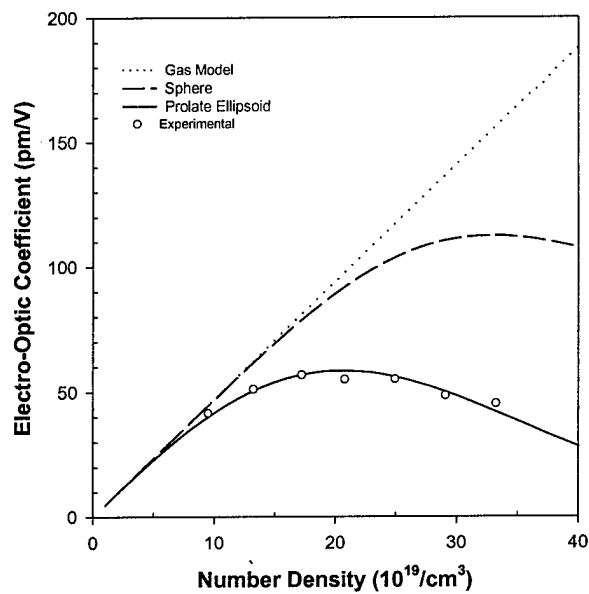


Fig. 2.1 Plot of theoretically predicted electro-optic coefficients versus number density for the FTC chromophore. For theoretical calculations, the molecules are treated as hard spheres or prolate ellipsoids.<sup>11</sup>

solved over many orientational variables. Instead, a coordinate system such as the one shown in Figure 2.2 is used to approximate the analytical solution.

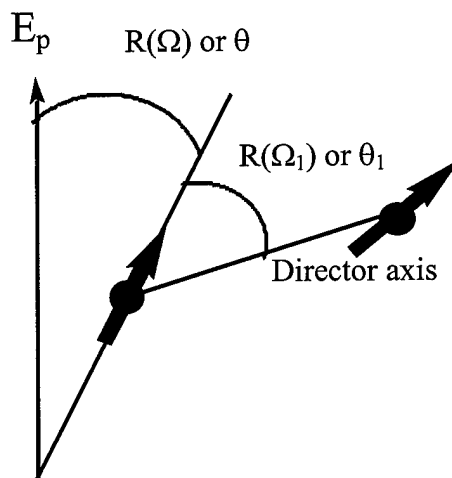


Fig. 2.2 The laboratory reference system used to relate chromophores to each other and to the electric field.  $R(\Omega)$  is the rotation matrix relating the reference chromophore to the laboratory axis.  $R(\Omega_1)$  is the rotation matrix for the interaction between the reference chromophore's principal axis and the director axis of other chromophores that contribute to the field felt by the reference chromophore.<sup>11</sup>

A reference chromophore is chosen and all other chromophores are arranged in a lattice around it, where the chromophore number density fixes all the distances. Now the reference chromophore in the center can be related to the electric poling field and the other chromophores. By choosing a director axis, all the chromophores that contribute to the field felt by the reference chromophore that can be included as a function of  $\Omega_i$ . An average is calculated over the orientational variables related to the other chromophores per Piekara, which is analogous to London's treatment.<sup>5,12</sup> The result gives an electrostatic interaction energy between chromophores,  $U_2$ , depending on one angle,  $\Omega$ . The equation is:

$$U_2 = -W \cos(\Omega_1) \quad (2.13)$$

The potential function used in the ordering parameter  $\langle \cos^3 \theta \rangle$  is then given by:

$$U = U_1 + U_2 = -\mu f_p E_p \cos \theta - W \cos(\theta_1) \quad (2.14)$$

By using the trigonometric identity:

$$\cos \theta = \cos \theta' \cos \theta_1 + \sin \theta' \sin \theta_1 \cos(\phi_1 - \phi') \quad (2.15)$$

the orientational integrals are easier to solve. Next, the chromophores are treated as hard spheres to give an expression for  $\langle \cos^3 \theta \rangle$  as:

$$\langle \cos^3 \theta \rangle = \left( \frac{\mu f_p E_p}{5kT} \right) \left[ 1 - L^2 \left( \frac{W}{kT} \right) \right] \quad (2.16)$$

where  $L$  is the Langevin function expressed in terms of  $W/kT$  and  $W$  is approximately the intermolecular electrostatic interaction energy given by London. As the concentration increases, the acentric order parameter decreases. Equation (2.16) verifies the maxima that appear in the plots of electro-optic coefficient versus chromophore number density. From Fig. 2.1 it would make sense to produce chromophores with spherical architecture, which has been done successfully by Dalton *et. al.*<sup>5</sup> proving the theoretical calculations correct.

## Notes to Chapter 2

1. Debye, P., *Phys. Z.*, 1935, **36**, 100-101.
2. Wang, F., Ph.D. Thesis, University of Southern California, 1998.
3. Zhang, C., Ph.D. Thesis, University of Southern California, 1999.
4. London, F., *Trans. Faraday Soc.*, 1937, **33**, 8-26
5. Dalton, L.R., Harper, A.W., Robinson, B.H., *Proc. Natl. Acad. Sci. USA*, 1997, **94**, 4842-4847.
6. Harper, A.W., Sun, S., Dalton, L.R., Garner, S.M., Chen, A., Kalluri, S., Steier, W.H., Robinson, B.H., *J. Opt. Soc. Amer. B*, 1998, **15**, 329-337.
7. Dalton, L.R., Harper, A.W., *Polym. News*, 1998, **23**, 114-120.
8. Healy, D., Thomas, P.R., Szablewski, M., Cross, G.H., *Proc. SPIE*, 1995, **2527**, 32-40.
9. Moylan, C.R., Miller, R.D., Twieg, R.J., Ermer, S., Lovejoy, S.M., Leung, D.S., *Proc. SPIE*, 1995, **2527**, 150-162.
10. Flipse, M.C., Van der Vorst, C.P.J.M., Hofstrant, J.W., Woudenberg, R.H., Van Gassel, R.A.P., Lamers, J.C., Van der Linden, E.G.M., Veenis, W.J., Diemeer, M.B.J., Donckers, M.C.J.M.. "Recent progress in polymer based electro-optic modulators: Materials and technology." In Photoactive Organic Materials: Science and Applications, eds. F. Kajzar, V.M. Agranovich, C.Y. -C. Lee, 25-30 June, 1995, Avignon, France, Kluwer Academic Publishers, Dordrecht, 1996, pp. 227-246.
11. Dalton, L.R., Steier, W.H., Robinson, B.H., Zhang, C., Ren, A., Garner, S., Chen, A., Londergan, T., Irwin, L., Carlson, B., Fifield, L., Phelan, G., Kincaid, C., Amend, J., Jen, A., *J. Mater. Chem.*, 1999, **9**, 1905-1920.
12. Piekara, A., *Proc. R. Soc. London A*, 1939, **149**, 360.

## Chapter 3

### Design and Synthesis of Chromophores Based on Reducing Intermolecular Electrostatic Interaction

#### 3.1 Introduction

##### 3.1.1 Motivation for Research

One of the biggest challenges in nonlinear optic material research is translating microscopic to macroscopic optical nonlinearity. A chromophore can be thermally and chemically stable, show low optical loss, display high  $\mu\beta$  values and still not reflect high  $r_{33}$  numbers in the chromophore/polymer composite material. As mentioned earlier, Dalton and coworkers discovered that dipole-dipole interactions among chromophores limit the degree of noncentrosymmetric order in the absence of chromophore modifications that sterically inhibit such interactions.<sup>1,2</sup> Last year Liakatas *et. al.*<sup>3</sup> and Shi *et. al.*<sup>4</sup> reported enhanced  $V_\pi$  and  $\mu\beta$  values based on bulky donor groups and modified bridges to reduce intermolecular electrostatic interactions.

#### 3.2 Design and Synthesis of the Chromophores

##### 3.2.1 Design and Synthesis of the Triphenylamine Donor

There are three reasons for choosing this particular donor structure. The first is that there is a need for bulky donor groups to sterically inhibit interactions with other chromophores. This donor should also not have any intramolecular H-bonding that would reduce the strength of the donor. The second reason is a result of a study by Marder and Perry<sup>5</sup> that showed an increase in  $\beta_0$  values, although slightly red-shifted, for di-aryl amine donors over di-alkyl amine donors, both attached to a phenyl group. The

third reason is a result of research done at IBM.<sup>6-10</sup> Workers there found an increase in thermal stability of amine donor groups by switching from alkyl amines to aryl amines. The donor synthesis was started with a variation of a one-pot palladium catalyzed amination published by Thayamanavan *et. al.*<sup>11</sup> The structure and synthetic pathway of the donor are shown in Figures 3.1 and 3.2.

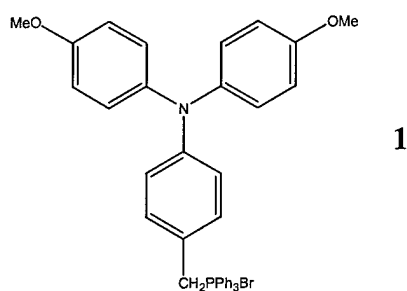


Fig. 3.1 Structure of Triphenylamine donor in Wittig salt form.

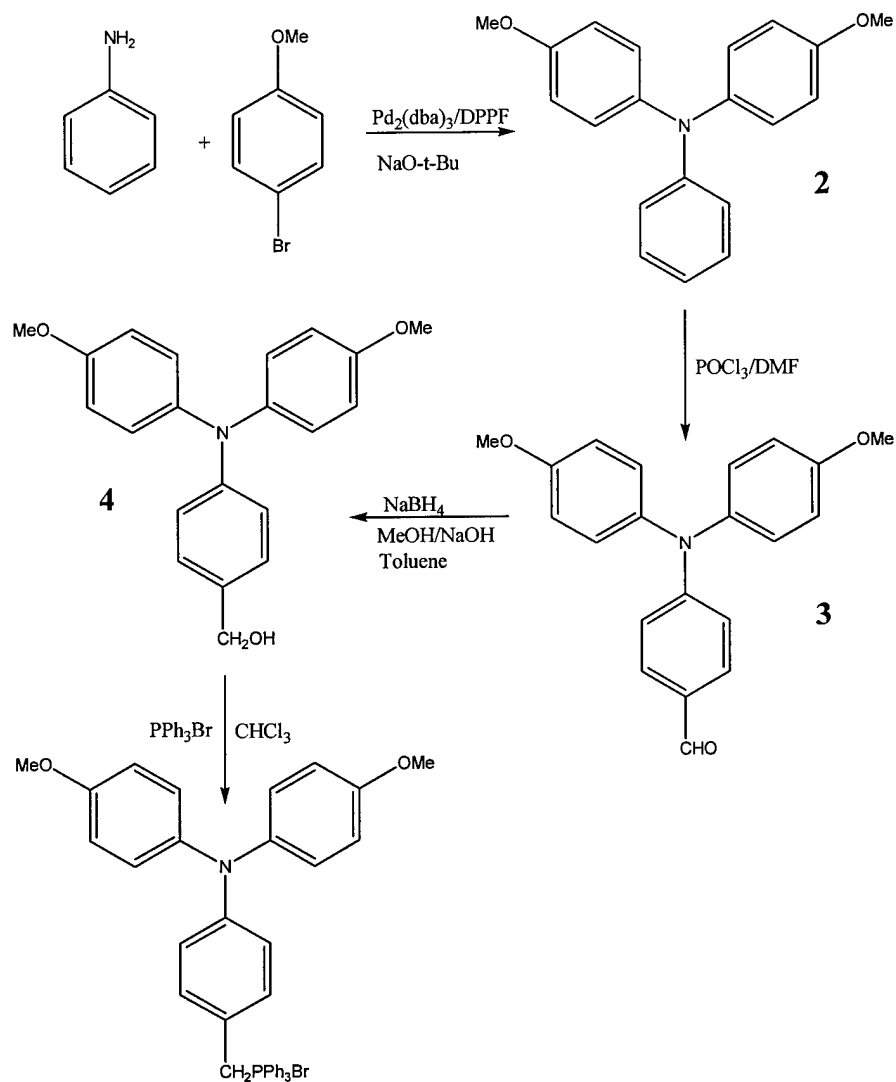


Fig. 3.2 Synthetic scheme for Triphenylamine Donor in Wittig salt form.

### 3.2.2 Design and Synthesis of Chromophores Based on Triphenylamine Donor

Each chromophore acceptor utilized the 2-dicyanomethylen-3-cyano-4,5,5-trimethyl-2,5dihydrofuran acceptor designed at Lockheed-Martin. Marder<sup>12-16</sup> and Jen<sup>17-20</sup> have also shown that polyene chain and thiophene-containing bridges give higher  $\beta$



values. Two chromophores were produced with the triphenylamine donor for comparison to two other similar chromophores containing different donors. Their structures are shown in Figures 3.2 and 3.3. The synthesis of the intermediates followed literature procedures with slight modifications as shown in Figures 3.4, 3.5 and 3.6.

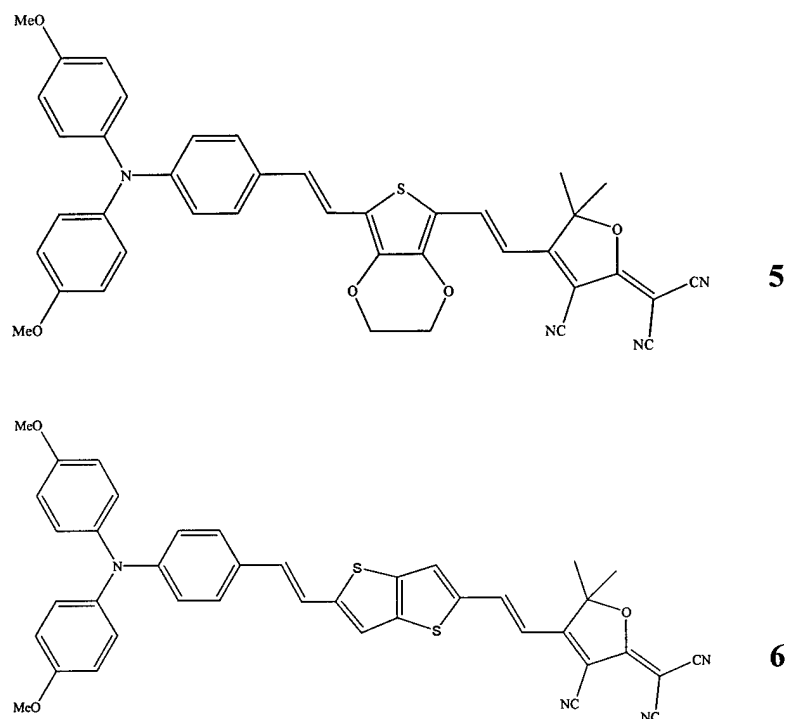


Fig. 3.2 Structures of the two chromophores with triphenylamine donors produced for this study.

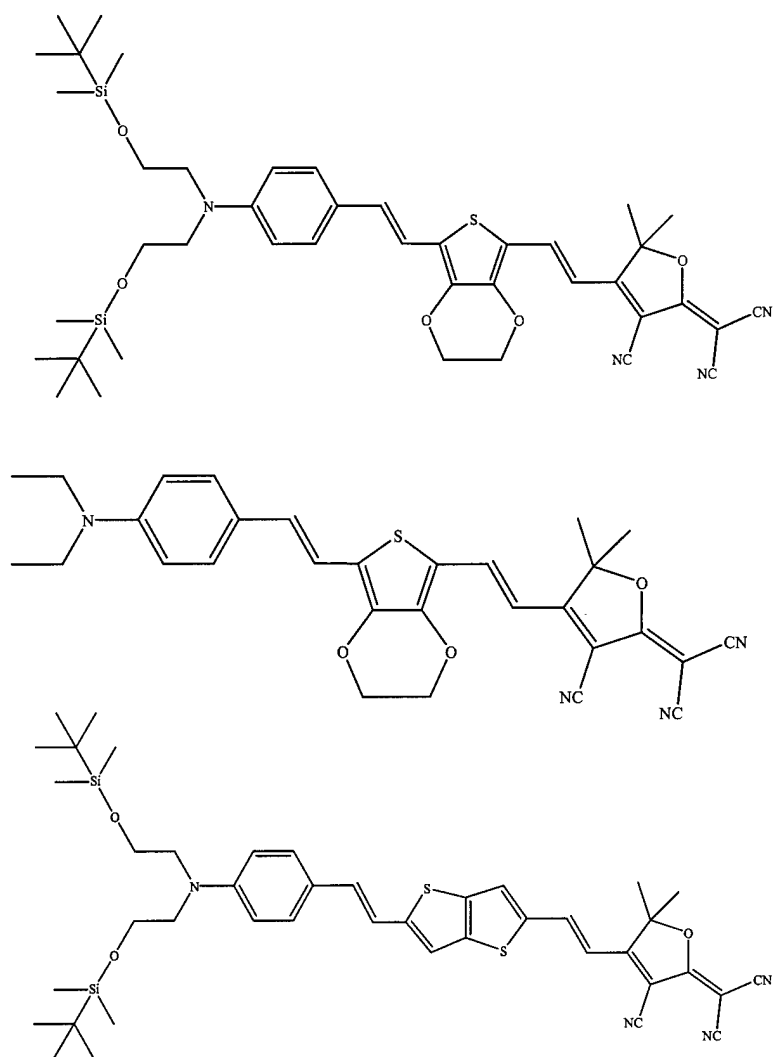


Fig. 3.3 Structures of 3 chromophores produced by other graduate students for comparison to triphenylamine donor chromophores.

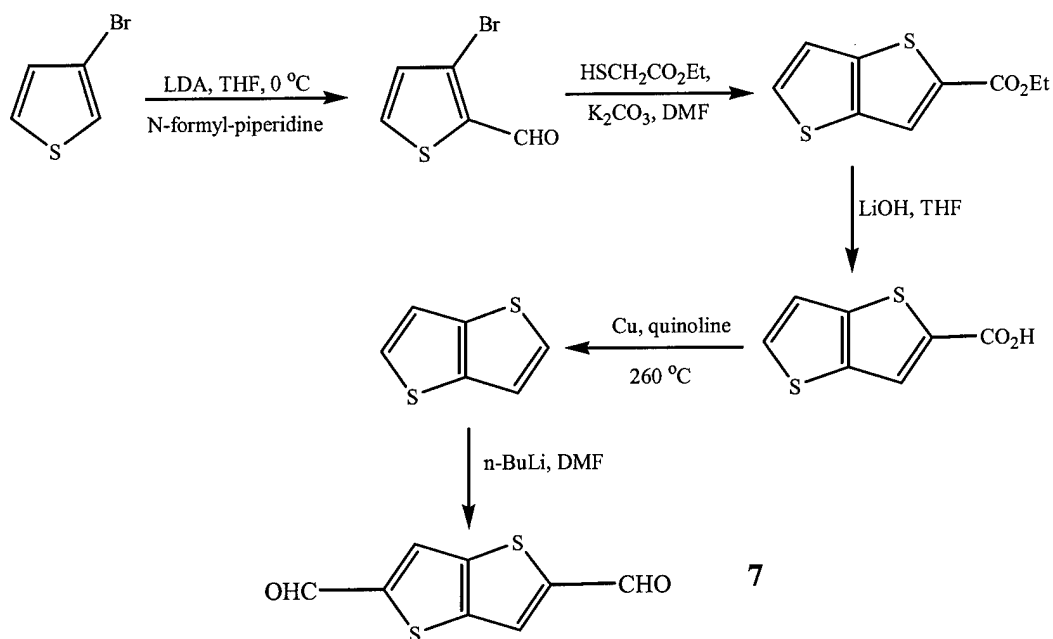


Fig. 3.4 Synthetic pathway for obtaining the dialdehyde version of thieno[3,2-b]thiophene for the bridge.

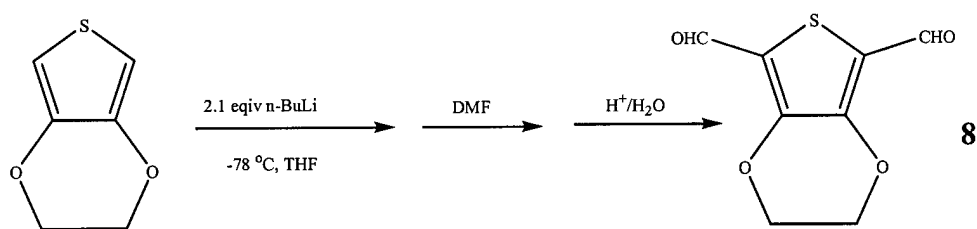


Fig. 3.5 Synthetic pathway for obtaining the bridge 2,3-thiopheno[3,4-e]1,4-dioxane-5,7-dicarbaldehyde

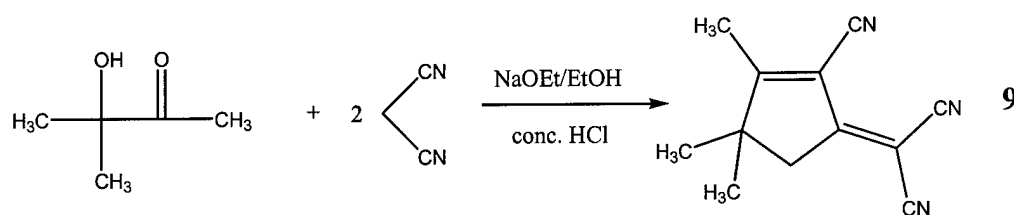


Fig. 3.6 Synthetic pathway for obtaining the 2-dicyanomethylen-3-cyano-4,5,5-trimethyl-2,5-dihydrofuran acceptor.

The synthetic schemes for the chromophores are shown in Figures 3.7 and 3.8.

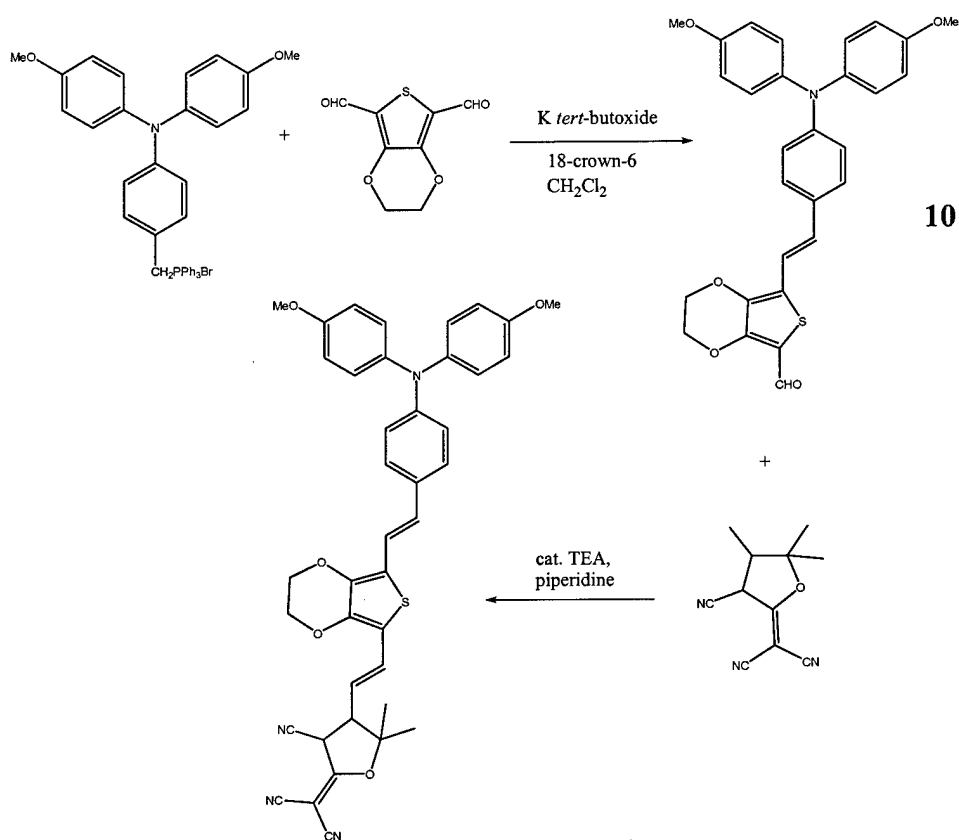


Fig. 3.7 Synthetic pathway for chromophore 5.

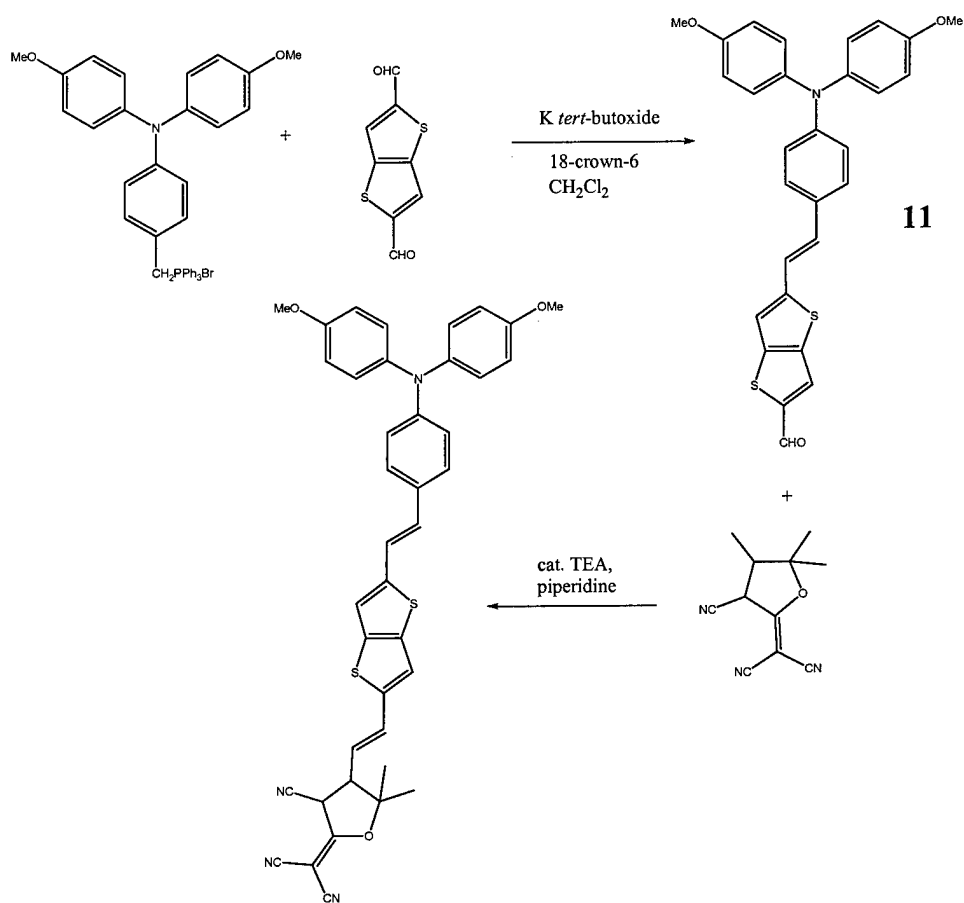


Fig. 3.8 Synthetic pathway for chromophore 6.

### 3.3 Experimental Section

#### 3.3.1 General Materials and Methods

The solvents and chemicals used were purchased from Aldrich, Acros and other chemical companies. They were analytical reagent grade unless otherwise noted. Column chromatography was performed on 70-230 mesh Lancaster silica gel 60. Conventional  $^1H$  NMR spectra were recorded using a Bruker 200 FT NMR spectrometer. The chemical shifts are referenced to tetramethylsilane (TMS) internal standard.

### 3.3.2 Synthesis of Bis-(4-methoxyphenyl){4-[(triphenylphosphonium bromide) methyl]phenyl}amine (1)

**Bis(4-methoxyphenyl)phenylamine (2):** The synthesis of the triphenylamine donor Wittig salt follows the schematic in Fig. 3.2. To a solution of 4.975g (5.43 mmol) of tris(dibenzylideneacetone)-dipalladium(0) and 4.519g (8.15mmol) of 1,1'-bis(diphenylphosphine)-ferrocene in 680mL toluene under nitrogen was added 68.46mL (0.245mol) of 4-bromoanisole and was allowed to stir for 25 minutes. Then, sodium *tert*-butoxide (59.36g, 0.618mol) and aniline (22.5mL, 0.236mol) were added to the solution and stirred at 90°C for approximately 2 weeks. Thin layer chromatography was used to monitor the complete formation of the decoupled product. The reaction solution was then worked up with brine washings (3x), extracted with ether, and dried over MgSO<sub>4</sub>. A flash column of 5% ethyl acetate/95% hexanes gave a light brown solid. The still crude product was purified on a column with 1% ethyl acetate/99% hexanes mobile phase to give 21.19g of white solid. <sup>1</sup>H NMR (CDCl<sub>3</sub>): δ3.87 (s, 6H), δ6.87-7.08 (m, 11H), δ7.26 (d, 2H).

**4-[bis(4-methoxyphenyl)amino]benzaldehyde (3):** In an addition funnel, 0.34mL (3.64mmol) of POCl<sub>3</sub> was added dropwise to a stirred cooled solution at 0°C containing 0.76mL (9.84mmol) of DMF in a three-neck flask and allowed to stir for one hour. The mixture was then allowed to warm to room temperature. A solution of **2** (1.0g, 3.28mmol) in 1,2 dichloroethane was then added dropwise. After complete addition, the additional funnel was replaced with a condenser and the solution was heated to 90-95°C for ~3 hours. After slight cooling, the solution was added dropwise to

a solution of  $\text{NaHCO}_3$ . The crude product was extracted with  $\text{CH}_2\text{Cl}_2$ , washed 3x with  $\text{NaHCO}_3$ , and dried over  $\text{Na}_2\text{SO}_4$ . The crude product was purified with column chromatography with 20% ethyl acetate/80%hexanes as the mobile phase to reveal 1.04g of viscous bright yellow oil.  $^1\text{H}$  NMR ( $\text{CDCl}_3$ ):  $\delta$ 3.99 (s, 6H),  $\delta$ 6.90 (d, 4H),  $\delta$ 7.20 (d, 4H),  $\delta$ 7.61 (d, 2H),  $\delta$ 9.79 (s, 1H).

**{4-[bis(4-methoxyphenyl)amino]phenyl}methan-1-ol (4):** To a solution of methanol, 14.9g (45 mmol) of **3** was added and stirred. To a prepared solution of 0.75g of NaOH in 2.5mL  $\text{H}_2\text{O}$  was added  $\text{NaBH}_4$  (0.85g, 22.5 mmol) and 25mL of methanol. The prepared solution was added to the stirred solution of **3** at  $0^\circ\text{C}$  via an addition funnel. The solution was allowed to stir at room temperature overnight. The solution was then worked up with brine washings (3x), extracted with ether, and dried over  $\text{MgSO}_4$ . Removal of solvent revealed 14.84g of dark orange oil. The product was used without further purification.  $^1\text{H}$  NMR ( $\text{CDCl}_3$ ):  $\delta$ 3.95 (s, 6H),  $\delta$ 4.73(s, 2H),  $\delta$ 6.94 (d, 4H)  $\delta$ 7.07 (d, 4H),  $\delta$ 7.20 (d, 2H),  $\delta$ 7.31 (d, 2H).

**Bis-(4-methoxyphenyl){4-[(triphenylphosphonium bromide)methyl]phenyl)amine (1):** A solution of **4** (14.84g, 0.044 mmol) and triphenylphosphonium hydrobromide (13.7g, 0.040 mmol) in 100mL of chloroform was placed on an azeotrope distillation apparatus and refluxed to remove water for 2-3 hours. Once cooled to room temperature, the chloroform solution was concentrated via rotary evaporation. The product was precipitated using ether and 27.8g were isolated by filtration. The  $^1\text{H}$  NMR is shown in Figure 3.9.  $^1\text{H}$  NMR ( $\text{CDCl}_3$ ):  $\delta$ 3.80 (s, 6H),  $\delta$ 5.22 (d, 2H),  $\delta$ 6.62 (d, 4H),  $\delta$ 6.79 (d, 4H),  $\delta$ 6.98 (d, 2H),  $\delta$ 7.60-7.81 (m, 15H).

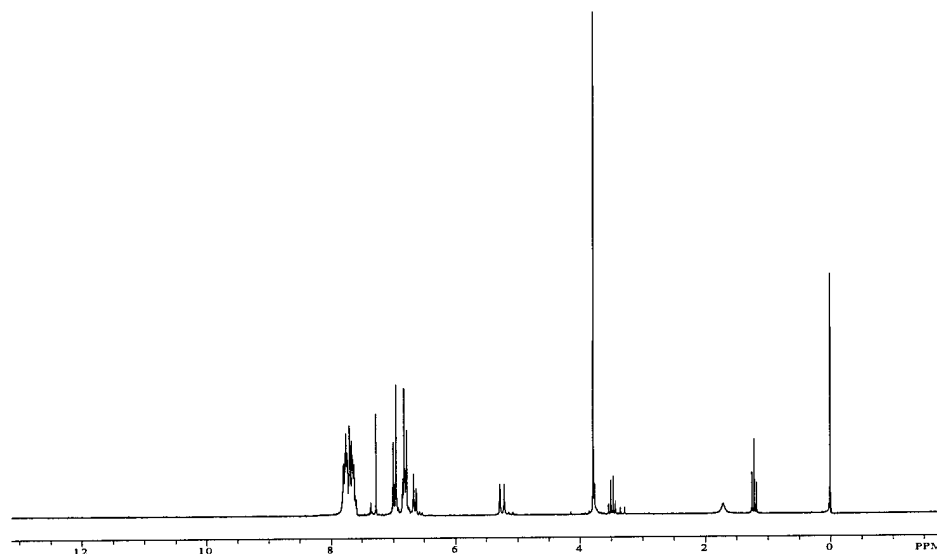


Fig. 3.9  $^1\text{H}$  NMR spectrum of triphenylamine donor Wittig salt

### 3.3.3 Synthesis of Chromophore 5

**Compound 10:** In a 1L round bottom flask, 6.67g (10.09 mmol) of **1** and 2.26g (20.14 mmol) of potassium *tert*-butoxide were added to about 300mL of methylene chloride. The solution was stirred vigorously for about two minutes at room temperature. Next, 83.70mg (0.32 mmol) of 18-crown-6 were added to 2g of **8** and stirred at room temperature for 2-3 hours. The solution was filtered over Celite and rotovaporated. Column chromatography using 5% ethyl acetate in hexane gave 1.1g of product.  $^1\text{H}$  NMR ( $\text{CDCl}_3$ ):  $\delta$ 3.91 (s, 6H),  $\delta$ 4.42-4.59 (m, 2H),  $\delta$ 6.91 (d, 4H),  $\delta$ 7.09 (d, 4H),  $\delta$ 6.99 (d, 2H),  $\delta$ 7.37 (d, 2H),  $\delta$ 7.41 (d, 1H),  $\delta$ 7.12 (d, 1H),  $\delta$ 10.18 (s, 1H),  $\delta$ 4.64 (q, 2H).



**Chromophore 5:** To compound **10** just enough chloroform to dissolve the product was added to a small vial with nearly 1g of **10**. The mixture was stirred and allowed to reflux. Then about 2-3 drops of triethylamine were added, and the solution continued to stir for about 30-45 minutes. It was quenched with ammonium chloride (2x) and washed with chloroform. It was then recrystallized in methanol and purified by column chromatography using 3% ethyl acetate in hexanes to afford 0.6g of product.  $^1\text{H}$  NMR ( $\text{CDCl}_3$ ):  $\delta$ 1.51 (s, 3H),  $\delta$ 1.62 (s, 3H),  $\delta$ 3.83 (s, 6H),  $\delta$ 4.42-4.53 (m, 4H),  $\delta$ 6.85 (d, 1H),  $\delta$ 6.90 (d, 4H),  $\delta$ 7.46 (d, 1H),  $\delta$ 7.13 (d, 1H).

### 3.3.4 Synthesis of Chromophore 6

**Compound 11:** In a 1L round bottom flask, 5.47g (8.28 mmol) of **1** and 1.86g (16.56 mmol) of potassium *tert*-butoxide were added to about 300mL of methylene chloride. The solution was stirred vigorously for about five minutes at room temperature. Next, 82.89mg (0.31 mmol) of 18-crown-6 were added to 2.5g of **7** and stirred at room temperature for 2-3 hours. The solution was filtered over Celite and roto-evaporated. Column chromatography using methylene chloride gave 0.9g of product.  $^1\text{H}$  NMR ( $\text{CDCl}_3$ ):  $\delta$ 3.84 (s, 6H),  $\delta$ 6.86 (d, 4H),  $\delta$ 6.83 (d, 4H),  $\delta$ 7.02 (d, 2H),  $\delta$ 7.31 (d, 1H),  $\delta$ 7.46 (d, 2H),  $\delta$ 8.02 (d, 1H),  $\delta$ 9.98 (s, 1H).

**Chromophore 6:** To compound **11** just enough chloroform to dissolve the product was added to a small vial with 0.86g of **11**. The mixture was stirred and allowed to reflux. Then about 2-3 drops of triethylamine were added, and the solution continued to stir for about 30-45 minutes. It was quenched with ammonium chloride (2x) and washed with chloroform. It was then recrystallized in methanol and purified by column

chromatography using methylene chloride to afford 0.55g of product.  $^1\text{H}$  NMR ( $\text{CDCl}_3$ ):  
 $\delta$ 1.56 (s, 3H),  $\delta$ 1.69 (s, 3H),  $\delta$ 3.92 (s, 6H),  $\delta$ 6.96 (d, 4H),  $\delta$ 6.85 (d, 4H),  $\delta$ 6.90 (d, 2H),  
 $\delta$ 8.24 (d, 1H),  $\delta$ 7.93 (d, 1H).

### 3.4 Conclusion

The bottom line for these syntheses is that the bulky donor unit is very easy to make and functionalize, if needed. We believe that it will offer more stability to the chromophore in both physical and thermal realms. With its shape, it will also somewhat inhibit intermolecular electrostatic interactions, and a little savings between the energy of the chromophores can go a long way concerning increased electro-optic coefficients.

### Notes to Chapter 3

1. Dalton, L.R., Steier, W.H., Robinson, B.H., Zhang, C., Ren, A., Garner, S., Chen, A., Londergan, T., Irwin, L., Carison, B., Leonard, F., Phelan, G., Kincaid, C., Amend, J., Jen, A., *J. Mater. Chem.*, 1999, **9**, 1905-1920.
2. Dalton, L.R., Harper, A.W., Robinson, B.H., *Proc. Natl. Acad. Sci. U.S.A.*, 1997, **94**, 4842.
3. Liakatas, I., Cai, C., Bosch, M., Jager, M., Bosshard, Ch., Gunter, P., Zhang, C., Dalton, L.R., *Applied Physics Letters*, 2000, **76**, 1368.
4. Shi, Y., Zhang, C., Zhang, H., Bechtel, J.H., Dalton, L.R., Robinson, B.H., Steier, W.H., *Science*, 2000, **288**, 119.
5. Harper, A.W., Ph.D. Thesis, University of Southern California, 1996.
6. Moylan, C.R., Miller, R.D., Twieg, R.J., Lee, V.Y., Characterization of nonlinear optical chromophores in solution, in *Polymers for Second-Order Nonlinear Optics*, eds. G.F. Lindsay, K.D. Singer, ACS Symp. Ser. 601, August 21-25, 1994, Washington, DC, American Chemical Society, Washington, DC, 1995, Chapter 5, pp. 66-81.
7. Miller, R.D., Moylan, C.R., Reiser, O., Walsh, C.A., *Chem. Mater.*, 1993, **5**, 625-632.
8. Twieg, R.J., Burland, D.M., Hedrick, J.L., Lee, V.Y., Miller, R.D., Moylan, C., Volksen, W., Walsh, C., *Mater. Res. Soc. Symp. Proc.*, 1994, **328**, 421-431.
9. Twieg, R.J., Betterton, K.M., Burland, D.M., Lee, V.Y., Miller, R.D., Moylan, C.R., Volksen, W., Walsh, C., *Proc. SPIE*, 1993, **2025**, 94-105.
10. Moylan, C.R., McComb, I.-H., Miller, R.D., Lee, V.Y., Twieg, R.J., *Mol. Cryst. Liq. Cryst.*, 1996, **283**, 115-118.
11. Thayumanavan, S., Barlow, S., Marder, S.R., *Chem. Mater.*, 1997, **9**, 3231-3235.
12. Marder, S.R., Beratan, D.N., Cheng, L.-T., *Science*, 1991, **252**, 103.
13. Tiemann, B.G., Marder, S.R., Cheng, L.-T., *J. Chem. Soc., Chem. Commun.*, 735, 1992.
14. Marder, S.R., Gorman, C.B., Cheng, L.-T., Tiemann, B.G., *Proc. SPIE*, 1992, **1775**, 19.

15. Gilmour, S., Marder, S.R., Perry, J.W., Cheng, L.-T., *Advanced Material*, 1994, **6**, 494.
16. Marder, S.R., Cheng, L.-T., Tiemann, B.G., Friedli, A.C., Blanchard-Desce, M., Perry, J.W., Skindhøj, J., *Science*, 1994, **263**, 511.
17. Drost, K.J., Jen, A.K.Y., Rao, V.P., *Chemtech*, 1995, **25**, 16.
18. Jen, A.K.Y., Wong, K.Y., Rao, V.P., Drost, K.J., Cai, Y.M., *J. Electronic Mater.*, 1994, **23**, 653.
19. Rao, V.P., Jen, A.K.Y., Wong, K.Y., Drost, K.J., *Tetrahedron Lett.*, 1993, **34**, 1747.
20. Jen, A.K.Y., Rao, V.P., Wong, K.Y., Drost, K.J., *J. Chem. Soc., Chem. Commun.*, 90, 1993.

## Bibliography

- Boldt, P., Bourhill, G., Brauchle, C., Jim, Y., Kammler, R., Muller, C., Rase, J., Wichern, J., *J. Chem. Commun.*, 1996, 793.
- Burland, D.M., Miller, R.D., Walsh, C.A., *Chem. Rev.*, 1994, **94**, 31.
- Chen, A., Ph.D. Dissertation, 1998, Department of Electrical Engineering, University of Southern California.
- Dalton, L.R., Steier, W.H., Robinson, B.H., Zhang, C., Ren, A., Garner, S., Chen, A., Londergan, T., Irwin, L., Carison, B., Leonard, F., Phelan, G., Kincaid, C., Amend, J., Jen, A., *J. Mater. Chem.*, 1999, **9**, 1905-1920.
- Dalton, L.R., *Kirk-Othmer Encyclopedia of Chemical Technology*, 4<sup>th</sup> edn., Vol. 17, Wiley, New York, 1996, p. 287.
- Dalton, L.R., Harper, A.W., Wu, B., Ghosn, R., Laquinadanum, J., Liang, Z., Hubbel, A., Xu, C., *Adv. Mater.*, 1995, **7**, 519.
- Dalton, L.R., Harper, A.W., Ghosn, R., Steier, W.H., Ziari, M., Fetterman, H.R., Shi, Y., Mustacich, R.V., Jen, A.K.Y., Shea, K.J., *Chem. Mater.*, 1995, **7**, 1060.
- Dalton, L.R., Harper, A.W., Robinson, B.H., *Proc. Natl. Acad. Sci. USA*, 1997, **94**, 4842-4847.
- Dalton, L.R., Harper, A.W., *Polym. News*, 1998, **23**, 114-120.
- Drost, K.J., Jen, A.K.Y., Rao, V.P., *Chemtech*, 1995, **25**, 16.
- Eldada, L., Blomquist, R., Shacklette, L.W., McFarland, M.J., *Opt. Eng.*, 2000, **39**, 596-609.
- Flipse, M.C., Van der Vorst, C.P.J.M., Hofstrant, J.W., Woudenberg, R.H., Van Gassel, R.A.P., Lamers, J.C., Van der Linden, E.G.M., Veenis, W.J., Diemeer, M.B.J., Donckers, M.C.J.M., "Recent progress in polymer based electro-optic modulators: Materials and technology." In *Photoactive Organic Materials: Science and Applications*, eds. F. Kajzar, V.M. Agranovich, C.Y. -C. Lee, 25-30 June, 1995, Avignon, France, Kluwer Academic Publishers, Dordrecht, 1996, pp. 227-246.
- Gilmour, S., Marder, S.R., Perry, J.W., Cheng, L.-T., *Advanced Material*, 1994, **6**, 494.
- Harper, A.W., Ph.D. Thesis, University of Southern California, 1996.

- Harper, A.W., Sun, S., Dalton, L.R., Garner, S.M., Chen, A., Kalluri, S., Steier, W.H., Robinson, B.H., *J. Opt. Soc. Amer. B*, 1998, **15**, 329-337.
- Healy, D., Thomas, P.R., Szablewski, M., Cross, G.H., *Proc. SPIE*, 1995, **2527**, 32-40.
- Jen, A.K.Y., Wong, K.Y., Rao, V.P., Drost, K.J., Cai, Y.M., *J. Electronic Mater.*, 1994, **23**, 653.
- Jen, A.K.Y., Rao, V.P., Wong, K.Y., Drost, K.J., *J. Chem. Soc., Chem. Commun.*, 90, 1993.
- Liakatas, I., Cai, C., Bosch, M., Jager, M., Bosshard, Ch., Gunter, P., Zhang, C., Dalton, L.R., *Applied Physics Letters*, 2000, **76**, 1368.
- London, F., *Trans. Faraday Soc.*, 1937, **33**, 8-26
- Marder, S.R., Cheng, L.-T., Tiemann, B.G., Friedli, A.C., Blanchard-Desce, M., Perry, J.W., Skindhøj, J., *Science*, 1994, **263**, 511.
- Marder, S.R., Gorman, C.B., Cheng, L.-T., Tiemann, B.G., *Proc. SPIE*, 1992, **1775**, 19.
- Marder, S.R., Beratan, D.N., Cheng, L.-T., *Science*, 1991, **252**, 103.
- Marks, T.J., Ratner, M., *Angew. Chem., Int. Ed. Engl.*, 1995, **34**, 155.
- Miller, R.D., Moylan, C.R., Reiser, O., Walsh, C.A., *Chem. Mater.*, 1993, **5**, 625-632.
- Moylan, C.R., McComb, I.-H., Miller, R.D., Lee, V.Y., Twieg, R.J., *Mol. Cryst. Liq. Cryst.*, 1996, **283**, 115-118.
- Moylan, C.R., Miller, R.D., Twieg, R.J., Lee, V.Y., Characterization of nonlinear optical chromophores in solution, in *Polymers for Second-Order Nonlinear Optics*, eds. G.F. Lindsay, K.D. Singer, ACS Symp. Ser. 601, August 21-25, 1994, Washington, DC, American Chemical Society, Washington, DC, 1995, Chapter 5, pp. 66-81.
- Moylan, C.R., Miller, R.D., Twieg, R.J., Ermer, S., Lovejoy, S.M., Leung, D.S., *Proc. SPIE*, 1995, **2527**, 150-162.
- Nalwa H.S., Miyata, S. Nonlinear Optics of Organic Molecules and Polymers, CRC Press, New York, 1997, p. 129.
- Nalwa H.S., Miyata, S. Nonlinear Optics of Organic Molecules and Polymers, CRC Press, New York, 1997, p. 406.

Nicoud, J.F., Twieg, R.J. in Nonlinear Optical Properties of Organic Molecules and Crystals, eds. D.S. Chemla, J. Zyss, Vol. 1, Academic Press, Orlando, 1989, p. 232.

Piekara, A., *Proc. R. Soc. London A*, 1939, **149**, 360.

Prasad, P.N., Williams, D.J. Introduction to Nonlinear Optical Effects in Molecules and Polymers, Wiley, New York, 1991.

Pugh, D., Morley, J.O. in Nonlinear Optical Properties of Organic Molecules and Crystals, eds. D.S. Chemla, J. Zyss, Vol. 1, Academic Press, Orlando, 1989, p. 205.

Rao, V.P., Jen, A.K.Y., Wong, K.Y., Drost, K.J., *Tetrahedron Lett.*, 1993, **34**, 1747.

Shi, Y., Ranon, P.M., Steier, W.H., Xu, C., Wu, B., Dalton, L.R., *App. Phys. Lett.*, 1993, **63**, 2168.

Shi, Y., Zhang, C., Zhang, H., Bechtel, J.H., Dalton, L.R., Robinson, B.H., Steier, W.H., *Science*, 2000, **288**, 119.

Tang, S., Shi, Z., An, D., Sun, L., Chen, R.T., *Opt. Eng.*, 2000, **39**, 680-688.

Thayumanavan, S., Barlow, S., Marder, S.R., *Chem. Mater.*, 1997, **9**, 3231-3235.

Tiemann, B.G., Marder, S.R., Cheng, L.-T., *J. Chem. Soc., Chem. Commun.*, 735, 1992.

Twieg, R.J., Betterton, K.M., Burland, D.M., Lee, V.Y., Miller, R.D., Moylan, C.R., Volksen, W., Walsh, C., *Proc. SPIE*, 1993, **2025**, 94-105.

Twieg, R.J., Burland, D.M., Hedrick, J.L., Lee, V.Y., Miller, R.D., Moylan, C., Volksen, W., Walsh, C., *Mater. Res. Soc. Symp. Proc.*, 1994, **328**, 421-431.

Wang, F., Ph.D. Thesis, University of Southern California, 1998.

Ward, *J. Rev. Mod. Phys.*, 1965, **37**, 1.

Wu, B., Xu, C., Dalton, L.R., Kalluri, S., Shi, Y., Steier, W.H., *Mater. Res. Soc. Symp. Proc.*, 1994, **328**, 529.

Xu, C., Wu, B., Becker, M.W., Dalton, L.R., Ranon, P.M., Shi, Y., Steier, W.H., *Chem. Mater.*, 1993, **5**, 1439.

Xu, C., Wu, B., Todorova, O., Dalton, L.R., Shi, Y., Ranon, P.M., Steier, W.H., *Macromolecules*, 1993, **26**, 5303.

Zernike, F., Midwinter, J.E. Applied Nonlinear Optics, Wiley, New York, 1973, p. 3ff.

Zhang, C., Ph.D. Thesis, University of Southern California, 1999.

Zhang, Y., Jen, A.K.Y., Chen, T., Liu, Y., Zhang, X., Kenney, J.T., *SPIE*, 1996, **3006**, 372.

Zhu, J., Ph.D. Thesis, University of Southern California, 1997.